Journal of Sound and Vibration (1997) **204**(2), 331–357

AN INTRODUCTION TO THE CONTROL OF SOUND FIELDS BY OPTIMISING IMPEDANCE LOCATIONS ON THE WALL OF AN ACOUSTIC CAVITY

V. Martin and A. Bodrero

Laboratoire de Mécanique de Rouen, *UPRESA CNRS* 6104, *INSA de Rouen*, *Avenue de l'Université*, *BP*08, 76801 *Saint Etienne du Rouvray*, *Cedex*, *France*

(*Received* 8 *August* 1996, *and in final form* 3 *February* 1997)

The paper presents a possible means of solving the problem of optimizing impedance locations on the walls of an acoustic cavity with rigid walls, when the goal is to reduce the sound level generated by a velocity source inside the cavity. First, an elementary analytical study of an academic situation shows how to deal with the problem. The methodology is then used on a finite element model of the cavity. Severe conditions constitute the framework because the situation is that of a large room (approx. 80 m^3) with a low frequency anti-resonance (arbitrarily around 70 Hz), with a limited number of pieces of absorptive material on the walls, called here impedances or impedance patches, and finally because the study begins with the search for optimal locations along a line on a face of the cavity. Under these conditions and until now, an attenuation of only a few dB has been obtained when the sound level minimization occurs at a small number of points, called here microphones, and less than one dB on a large number of microphones. Upon taking into consideration the narrow framework, these results encourage more extensive investigations.
© 1997 Academic Press Limited

1. ORIGIN OF THE SUBJECT AND INTRODUCTORY APPROACH

When an external sound source radiates noise inside a cavity with yielding walls, the sound level can be reduced by passive means such as improving the acoustic insulation of walls (weighting or doubling them) and damping the cavity (installing resonators or absorptive material), or with the help of active means such as active acoustic control (where loudspeakers are the secondary source) or active structural acoustic control (where actuators on the structure reduce the noise radiated), or by using both means. Here, control has to reduce sound level in an acoustic cavity coupled with a vibratory structure—its external radiation is not to be taken into consideration in the present context—representing a moving vehicle, particularly the satellite compartment of the Ariane 5 launcher.

Attenuation techniques are well-known, at least for a stationary deterministic field. Specific constraints for vehicles concern transported hardware, i.e., weight and volume. Concerning active acoustic control, the secondary sources are usually voluminous, need electrical supply and digital or analog systems for signal processing on racks. With this in mind and in an acoustic–structure coupling similar to the one here, it has already been shown that selection strategies and source location optimization result in limiting the number of sources, with a given attenuation to be reached [1–3]. For passive techniques, weight and volume also exist, leading one to try a transposition of location optimization from the active acoustic control domain to the passive acoustic control domain. Some

0022–460X/97/270331 + 27 $25.00/0/sv970963 © 1997 Academic Press Limited

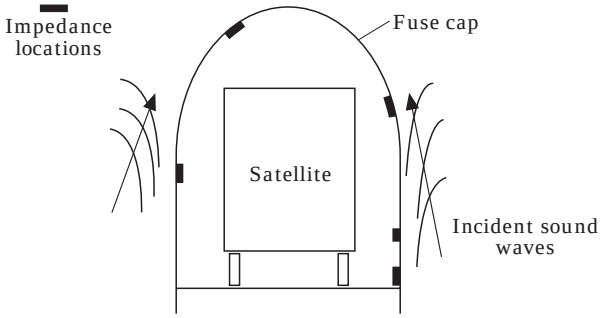

Figure 1. Motivation of the study.

authors have published work on the effects of impedance locations on the acoustic field in a cavity, when the impedances originate from Helmholtz resonators (see, e.g. references [4, 5]), but their goal was not location optimization by conventional gradient processing, which constitutes the purpose of the present paper.

More precisely the question is as follows: is it possible to optimize the location and number of passive absorbing devices, given their geometrical dimensions and their admittances, in order to minimize, in a cavity with yielding walls, the acoustic level caused by an external source? To this end, how can continuous optimization processing with a limited number of available measurements be used?

The proposed deterministic and harmonic approach is a cornerstone of the study concerning the satellite compartment of the Ariane 5 launcher, but it cannot constitute the entire approach. Indeed the passive devices currently used act partly with non-linear phenomena and the actual external excitation is, in its simplest form, random and stationary. Figure 1 shows the motivation for the present study and Figure 2 gives an elementary configuration of the actual situation.

The paper presents the approach to the problem in two steps. First, an analytical technique in a half-space indicates the natural path: integral formulation with a simple layer approximated by collocation and then by an asymptotic form, giving access to solutions of the optimization from an infinite number of data, called here measurements. The analytical form was also the starting point for reflection on how results could be obtained from a finite number of measurements. Some results have already been published [6, 7] but the methodology is further developed in this paper.

Thus Figure 2, modified by the fact that all the walls are rigid and that the source acts inside the cavity, is at the centre of the description. Variational formulation is followed by finite element discretization, a sub-structuring of the finite element matrix providing a form very similar to that of the analytical. Collocation, seen as some average values of

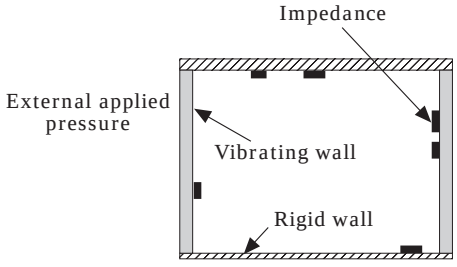

Figure 2. Elementary configuration.

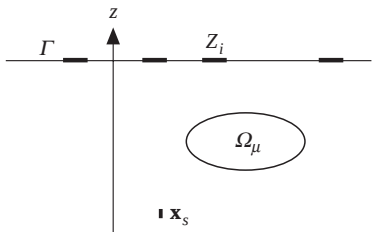

Figure 3. Academic situation.

the finite element form, and measurements are intricately related. The idea stemming from the analytical method, of working with a limited number of measurements is then transposed to the numerical model. The development of these measurements—also called sampled data—into Taylor series provides estimates of the functional under study, i.e., the acoustic level, and its first derivatives according to the impedance locations, whatever they are. A conventional gradient algorithm then has to minimize the level. Here also some results have already been presented [8] but once again including the work to be presented here provides a deeper insight into this introductory approach and gives more results.

2. ANALYTICAL FORMULATION OF AN ACADEMIC SITUATION

2.1. DIFFERENTIAL PROBLEM AND CALCULATION BY A BOUNDARY INTEGRAL METHOD

The simplest problem found to deal with absorptive device locations is in a three-dimensional half-space. Consider a simple acoustic source of given radial velocity situated at $\mathbf{x}_s$ and radiating in the three-dimensional half-space defined by $z \leqslant 0$ (cf. Figure 3).

The boundary that limits the 3-D half-space is the plane Γ defined by $z = 0$. On this non-vibrating plane, absorptive devices are installed. They may be absorptive material or Helmholtz resonators, and they are going to be considered throughout all the text as areas Z_i of admittance β_i. The reader will also recognize them as impedances or impedance patches.

An impedance patch is described by its area Z and the equation $\partial_n p(x) + \mathrm{i}k\beta p(x) = 0$ where p and $\partial_n p$ are respectively the acoustic pressure and its normal derivative on the impedance. The normal is directed outwards from the acoustic domain, here in the $z > 0$ direction, and k is the acoustic wavenumber.

An elementary example illustrates this type of equation. If the device comprises a vibrating piston composed of a mass m, a stiffness constant r, and a damping coefficient c, it vibrates under the action of the acoustic pressure p applied on it and its normal displacement satisfies $(-m\omega^2 + \mathrm{i}\omega c + r)u_n = pZ$. When adding the coupling with the acoustic domain through the displacement by saying that the air particles move like the piston at the interface, the acoustic dynamic equation is $\partial_n p = \rho\omega^2 u_n$ on Z. Eliminating the displacement between the two equations results in $\partial_n p + \mathrm{i}k\beta p = 0$ on Z where $\beta = \rho c Z\omega/[c\omega + \mathrm{i}(m\omega^2 - r)]$.

Everywhere on Γ except on the impedance patches Z_i, written as $\Gamma \backslash Z_i$, the rigid behavior is described by $u_n = 0$: that is, $\partial_n p = 0$.

In the acoustic space, the waves satisfy the wave equation, i.e., the Helmholtz equation

for a sinusoidal wave, written in the complex domain with a time dependence $e^{+i\omega t}$. The source velocity is such that the right side of the Helmholtz equation is -1.

Thus, the direct problem (see Figure 3) consists of finding the acoustic pressure $p(x)$ such that $(\Delta + k^2)p(\mathbf{x}) = -\delta(\mathbf{x} - \mathbf{x}_s)$ inside the half-space Ω defined by $z < 0$, $\partial_n p = 0$ on $\Gamma \backslash Z_t$ where $Z_t \equiv Z_1 \cup Z_2 \cup \cdots \cup Z_{N\zeta}$ if there are N_ζ impedance patches, $\partial_n p + ik\beta p = 0$ on Z_t, and $\lim_{r\to\infty} r(\partial_r p + ikp) = 0$.

This type of problem is solved by taking advantage of the known elementary solution which satisfies almost all the same equations, in particular the Helmholtz equation in the acoustic domain. Indeed, let $G(\mathbf{x}, \mathbf{x}')$ be the solution of $(\Delta_{\mathbf{x}} + k^2)G(\mathbf{x}, \mathbf{x}') = -\delta(\mathbf{x} - \mathbf{x}')$ inside the half-space Ω defined by $z < 0$, $\partial_n G = 0$ on Γ with no impedance on Γ, and $\lim_{r\to\infty} r(\partial_r p + ikp) = 0$

The elementary solution is itself built from the known elementary solution in the entire 3-D space, that has the form $e^{-ikr}/4\pi r$ where r is the distance between source and observer. The perfectly rigid boundary Γ is a perfect mirror on which acoustic waves radiated by the source reflect, as if the reflecting waves were originating from the image source of the true source through the mirror. The total solution is the sum of the waves generated by the true source and its image as indicated on Figure 4. Thus, $G(\mathbf{x}, \mathbf{x}')$ is $(e^{-ikr_1}/4\pi r_1) + (e^{-ikr_2}/4\pi r_2)$ and $r_1 = r_2 = r$ when $\mathbf{x}$ and/or $\mathbf{x}'$ are on Γ, leading to

$$G(\mathbf{x}, \mathbf{x}') = \frac{e^{-ikr}}{2\pi r}.$$

What is called the Green theorem is the key to obtaining the pressure p from the elementary solution $G(\mathbf{x}, \mathbf{x}')$. Denoting $H = (\Delta_x + k^2)$ and for $x \in \Omega$, one has

$$\int_\Omega (GHp - pHG)\, d\Omega = -\int_\Omega G(\mathbf{x}, \mathbf{x}')\, \delta(\mathbf{x} - \mathbf{x}_s)\, d\mathbf{x} + \int_\Omega p(x)\, \delta(\mathbf{x} - \mathbf{x}')\, d\mathbf{x}.$$

Integration by parts will reveal the boundary conditions. The boundary $\partial\Omega$ of the domain Ω is composed of the plane Γ with the impedance patches and of a fictitious hemispherical boundary as distant as possible from the domain of interest. On this fictitious boundary, both p and G satisfy the same condition, called the Sommerfield condition, which says that the waves reaching the hemispherical boundary propagate through it and never return. Notice that at the points where Γ meets the hemispherical boundary, things are not quite so clear since at such points two different conditions co-exist. This is because these points, as far as possible from the domain, have no influence on the solution p and so they are ignored. Upon taking into account what has been said, the integration by parts leads to

$$\int_\Omega (GHp - pHG)\, d\Omega = \int_\Gamma [G(\mathbf{x}, \mathbf{x}')\partial_n p(\mathbf{x}) - p(\mathbf{x})\partial_n G(\mathbf{x}, \mathbf{x}')]\, d\mathbf{x},$$

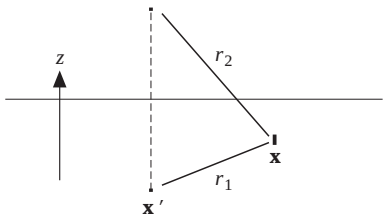

Figure 4. Image source method.

i.e.,

$$-G(\mathbf{x}_s, \mathbf{x}') + p(\mathbf{x}') = = \int_\Gamma [G(\mathbf{x}, \mathbf{x}')\partial_n p(\mathbf{x}) - p(\mathbf{x})\partial_n G(\mathbf{x}, \mathbf{x}')]\, \mathrm{d}\mathbf{x},$$

and, with $\mathbf{x}$ and $\mathbf{x}'$ playing the same role in G, this results in

$$p(\mathbf{x}) = G(\mathbf{x}, \mathbf{x}_s) + \int_\Gamma [G(\mathbf{x}, \mathbf{x}')\partial_n p(\mathbf{x}') - p(\mathbf{x}')\partial_{n'} G(\mathbf{x}, \mathbf{x}')]\, \mathrm{d}\mathbf{x}'.$$

Finally with $\partial_n G = 0$ on Γ and $\partial_n p = 0$ on $\Gamma \backslash Z_t$;

$$p(\mathbf{x}) = G(\mathbf{x}, \mathbf{x}_s) + \int_{Z_t} G(\mathbf{x}, \mathbf{x}')\partial_{n'} p(\mathbf{x}')\, \mathrm{d}\mathbf{x}' = G(\mathbf{x}, \mathbf{x}_s) - \mathrm{i}k\beta \int_{Z_t} G(\mathbf{x}, \mathbf{x}')p(\mathbf{x}')\, \mathrm{d}\mathbf{x}'. \quad (1)$$

Suppose that $\partial_n p$ were imposed on Z_t. The solution $p(\mathbf{x})$ with $\mathbf{x} \in \Omega$ would originate from two types of sources: the source inside the domain Ω which gives $G(\mathbf{x}, \mathbf{x}_s)$ and a continuous set of velocity sources (since $\partial_n p$ and the velocity v_n are linked through the dynamic acoustic equation) on Z_t. In fact the latter sources depend on the pressure in Ω and on Z_t. As only $G(\mathbf{x}, \mathbf{x}')$ appears in the boundary integral, the integral describing a single layer of sources is called a simple layer integral and equation (1) is true for $\mathbf{x} \in \Omega \cup \Gamma$.

2.2. APPROXIMATION BY COLLOCATION

With one impedance only and with the hypothesis that $p(\mathbf{x}_\zeta) = p_\zeta$ has a constant value on Z, form (1) has now become

$$p(\mathbf{x}) \approx G(\mathbf{x}, \mathbf{x}_s) - \mathrm{i}k\beta p(\mathbf{x}_\zeta) \int_Z G(\mathbf{x}, \mathbf{x}')\, \mathrm{d}\mathbf{x}'$$

which can be written as

$$p_x \approx p_{x0} - \mathrm{i}k\beta \left(\int_Z G(\mathbf{x}, \mathbf{x}')\, \mathrm{d}\mathbf{x}' \right) p_\zeta. \quad (2)$$

When $\mathbf{x} \to \mathbf{x}_\zeta$, it follows $p_\zeta \approx (1 + \mathrm{i}k\beta \int_Z G(\mathbf{x}_\zeta, \mathbf{x}')\, \mathrm{d}\mathbf{x}')^{-1} p_{\zeta 0}$, whence

$$p_{\mathbf{x}} \approx p_{\mathbf{x}0} - \mathrm{i}k\beta \left(\int_Z G(\mathbf{x}, \mathbf{x}')\, \mathrm{d}\mathbf{x}' \right) \left(1 + \mathrm{i}k\beta \int_Z \mathrm{G}(\mathbf{x}_\zeta, \mathbf{x}')\, \mathrm{d}\mathbf{x}' \right)^{-1} p_{\zeta 0}. \quad (3)$$

In view of the aim of this paper, it is fundamental to notice at this stage of the procedure that the pressure in Ω with impedance patches on Γ can be predicted from data in Ω without patches on Γ: i.e., with Γ perfectly rigid everywhere ($\partial_n p = 0$). When Ω is that of a vehicle, its boundary $\partial\Omega$, possibly vibrating but without linings such as trim panels in aircraft for example, will play the same role as that of Γ, without linings.

With two impedances ($Z_t = Z_1 \cup Z_2$), and with the same hypothesis, form (1) becomes

$$p(\mathbf{x}) \approx G(\mathbf{x}, \mathbf{x}_s) - \mathrm{i}k\beta p(\mathbf{x}_{\zeta_1}) \int_{Z_1} G(\mathbf{x}, \mathbf{x}')\, \mathrm{d}\mathbf{x}' - \mathrm{i}k\beta p(\mathbf{x}_{\zeta_2}) \int_{Z_2} G(\mathbf{x}, \mathbf{x}')\, \mathrm{d}\mathbf{x}',$$

which can be written as

$$p_{\mathbf{x}} \approx p_{\mathbf{x}0} - \mathrm{i}k\beta\left(\int_{Z_1} G(\mathbf{x}, \mathbf{x}')\,\mathrm{d}\mathbf{x}'\right)p_{\zeta_1} - \mathrm{i}k\beta\left(\int_{Z_2} G(\mathbf{x}, \mathbf{x}')\,\mathrm{d}\mathbf{x}'\right)p_{\zeta_2},$$

or

$$p_{\mathbf{x}} \approx p_{\mathbf{x}0} - \left\langle \mathrm{i}k\beta \int_{Z_1} G(\mathbf{x}, \mathbf{x}')\,\mathrm{d}\mathbf{x}', \mathrm{i}k\beta \int_{Z_2} G(\mathbf{x}, \mathbf{x}')\,\mathrm{d}\mathbf{x}' \right\rangle \begin{Bmatrix} p_{\zeta_1} \\ p_{\zeta_2} \end{Bmatrix}, \tag{4}$$

where $\langle . , . \rangle$ represents a row vector and $\{:\}$ a column vector.

When $\mathbf{x} \to \mathbf{x}_{\zeta_1}$, it follows that $p_{\zeta_1} \approx p_{\zeta_1 0} - \mathrm{i}k\beta(\int_{Z_1} G(\mathbf{x}_{\zeta_1}, \mathbf{x}')\,\mathrm{d}\mathbf{x}')p_{\zeta_1} - \mathrm{i}k\beta(\int_{Z_2} G \times (\mathbf{x}_{\zeta_1}, \mathbf{x}')\,\mathrm{d}\mathbf{x}')p_{\zeta_2}$.

When $\mathbf{x} \to \mathbf{x}_{\zeta_2}$, it follows that $p_{\zeta_2} \approx p_{\zeta_2 0} - \mathrm{i}k\beta(\int_{Z_1} G(\mathbf{x}_{\zeta_2}, \mathbf{x}')\,\mathrm{d}\mathbf{x}')p_{\zeta_1} - \mathrm{i}k\beta(\int_{Z_2} G(\mathbf{x}_{\zeta_2}, \mathbf{x}') \times \mathrm{d}\mathbf{x}')p_{\zeta_2}$, or

$$\begin{bmatrix} 1 + \mathrm{i}k\beta \int_{Z_1} G(\mathbf{x}_{\zeta_1}, \mathbf{x}')\,\mathrm{d}\mathbf{x}' & \mathrm{i}k\beta \int_{Z_2} G(\mathbf{x}_{\zeta_1}, \mathbf{x}')\,\mathrm{d}\mathbf{x}' \\ \mathrm{i}k\beta \int_{Z_1} G(\mathbf{x}_{\zeta_2}, \mathbf{x}')\,\mathrm{d}\mathbf{x}' & 1 + \mathrm{i}k\beta \int_{Z_2} G(\mathbf{x}_{\zeta_2}, \mathbf{x}')\,\mathrm{d}\mathbf{x}' \end{bmatrix} \begin{Bmatrix} p_{\zeta_1} \\ p_{\zeta_2} \end{Bmatrix} = \begin{Bmatrix} p_{\zeta_1 0} \\ p_{\zeta_2 0} \end{Bmatrix},$$

whence

$$p_{\mathbf{x}} \approx p_{\mathbf{x}0} - \left\langle \mathrm{i}k\beta \int_{Z_1} G(\mathbf{x}, \mathbf{x}')\,\mathrm{d}\mathbf{x}', \mathrm{i}k\beta \int_{Z_2} G(\mathbf{x}, \mathbf{x}')\,\mathrm{d}\mathbf{x}' \right\rangle \times \begin{bmatrix} 1 + \mathrm{i}k\beta \int_{Z_1} G(\mathbf{x}_{\zeta_1}, \mathbf{x}')\,\mathrm{d}\mathbf{x}' & \mathrm{i}k\beta \int_{Z_2} G(\mathbf{x}_{\zeta_1}, \mathbf{x}')\,\mathrm{d}\mathbf{x}' \\ \mathrm{i}k\beta \int_{Z_1} G(\mathbf{x}_{\zeta_2}, \mathbf{x}')\,\mathrm{d}\mathbf{x}' & 1 + \mathrm{i}k\beta \int_{Z_2} G(\mathbf{x}_{\zeta_2}, \mathbf{x}')\,\mathrm{d}\mathbf{x}' \end{bmatrix}^{-1} \begin{Bmatrix} p_{\zeta_1 0} \\ p_{\zeta_2 0} \end{Bmatrix}, \tag{5}$$

and so the knowledge of what happens when Γ is perfectly rigid allows one to predict what is going to happen when Γ is lined with impedance patches. For the sake of simplicity, equation (5) can be written in the form

$$p_{\mathbf{x}} \approx p_{\mathbf{x}0} - \mathrm{i}k\beta\langle \mathscr{G}(\mathbf{x}, \mathbf{x}_{\zeta_i})\rangle [I_{ij} + \mathrm{i}k\beta \mathscr{G}(\mathbf{x}_{\zeta_i}, \mathbf{x}_{\zeta_j})]^{-1}\{p_{\zeta_j 0}\}.$$

2.3. MINIMIZATION OF THE SOUND LEVEL FROM AN INFINITY OF "MEASUREMENTS"

2.3.1. *Asymptotic integral form and spot "measurements"*

Consider one sole impedance. The asymptotic form of equation (2) is obtained when $\mathbf{x} = \mathbf{x}_\mu$ is "far" from the impedance and when Z is "small". Indeed, with $\mathbf{x}_\zeta$ the

impedance centre,

$$f(\mathbf{x}) = \frac{1}{2\pi}\int_Z \frac{\mathrm{e}^{-\mathrm{i}k|\mathbf{x}-\mathbf{x}'|}}{|\mathbf{x}-\mathbf{x}'|}p(\mathbf{x}')\,\mathrm{d}\mathbf{x}' \approx \frac{p(\mathbf{x}_\zeta)}{2\pi}\int_Z \frac{\mathrm{e}^{-\mathrm{i}k|\mathbf{x}-\mathbf{x}'|}}{|\mathbf{x}-\mathbf{x}'|}\,\mathrm{d}\mathbf{x}'$$

and if $\mathbf{x}$ is far from $\mathbf{x}'|\mathbf{x}-\mathbf{x}'|$ hardly varies on $\mathbf{Z}$ as $\mathbf{x}'$ sweeps across Z, resulting in $f(\mathbf{x}) \approx (p(\mathbf{x}_\zeta)Z/2\pi)\,\mathrm{e}^{-\mathrm{i}k|\mathbf{x}-\mathbf{x}_\zeta|}/|\mathbf{x}-\mathbf{x}_\zeta|$, and thus

$$p(\mathbf{x}) = p_0(\mathbf{x}) - \mathrm{i}k\beta(Z/2\pi)\,\mathrm{e}^{-\mathrm{i}kd_{.\zeta}}/\mathrm{d}_{.\zeta}\,p(\mathbf{x}_\zeta), \quad \text{with} \quad \mathrm{d}_{.\zeta} = |\mathbf{x}-\mathbf{x}_\zeta|. \tag{6}$$

$p(\mathbf{x}_\zeta)$ is accessible when $\mathbf{x}\in Z\to\mathbf{x}_\zeta$: i.e., $d\to 0$. Indeed the integral $f(\mathbf{x})$ calculated in the vicinity of $\mathbf{x}_\zeta$ is

$$\lim_{r\to 0}\int_Z \frac{\mathrm{e}^{-\mathrm{i}kr}}{r}\,\mathrm{d}r = \lim_{r\to 0}\int_{\theta R(\theta)}\int r\,\mathrm{d}r\,\mathrm{d}\theta\,\frac{\mathrm{e}^{-\mathrm{i}kr}}{r} = P, \quad \text{whence} \quad p_0(\mathbf{x}_\zeta) = \left(1 + \mathrm{i}k\beta\,\frac{P}{2\pi}\right)p(\mathbf{x}_\zeta),$$

with P, the impedance perimeter when circular (for a square impedance, $P = 3{\cdot}52a$, where a is the side of the square). As a reminder: $p_0(\mathbf{x}_\zeta)$ or p_{ζ_0} is the pressure at the impedance location but without the impedance; $p(\mathbf{x})$ or $p_\mathbf{x}$ is the pressure at $\mathbf{x}$ with the impedance present; $p(\mathbf{x}_\zeta)$ or p_ζ is the pressure at the impedance location with the impedance present.

The asymptotic form of the integral equation (3) is thus

$$p(\mathbf{x}_\mu) = p_0(\mathbf{x}_\mu) - \mathrm{i}k\beta\left(\frac{Z}{2\pi}\,\frac{\mathrm{e}^{-\mathrm{i}kd_{\mu\zeta}}}{d_{\mu\zeta}}\right)\left(1 + \mathrm{i}k\beta\,\frac{P}{2\pi}\right)^{-1} p_0(\mathbf{x}_\zeta). \tag{7}$$

In the case of a number N_ζ of impedances, $Z_t = Z_1 \cup Z_2 \cup Z_3 \cdots \cup Z_{N\zeta}$. In particular with two impedances Z_1 and Z_2 of which the centres are $\mathbf{x}_{\zeta_1}$ and $\mathbf{x}_{\zeta_2}$, equation (1) becomes

$$p(\mathbf{x}) = G(\mathbf{x},\mathbf{x}_s) - \mathrm{i}k\beta\int_{Z_1} G(\mathbf{x},\mathbf{x}')p(\mathbf{x}')\,\mathrm{d}\mathbf{x}' - \mathrm{i}k\beta\int_{Z_2} G(\mathbf{x},\mathbf{x}')p(\mathbf{x}')\,\mathrm{d}\mathbf{x}',$$

and for "small" Z_1 and Z_2,

$$p(\mathbf{x}) \approx G(\mathbf{x},\mathbf{x}_s) - \mathrm{i}k\beta p(\mathbf{x}_{\zeta_1})\int_{Z_1} G(\mathbf{x},\mathbf{x}')\,\mathrm{d}\mathbf{x}' - \mathrm{i}k\beta p(\mathbf{x}_{\zeta_2})\int_{Z_2} G(\mathbf{x},\mathbf{x}')\,\mathrm{d}\mathbf{x}'.$$

Also, one knows that for $\mathbf{x}$ far from $\mathbf{x}_{\zeta_1}$ and $\mathbf{x}_{\zeta_2}$, $\int_{Z_i} G(\mathbf{x},\mathbf{x}')\,\mathrm{d}\mathbf{x}' \approx (Z_i/2\pi)\,\mathrm{e}^{-\mathrm{i}kd_{\zeta_i}}/d_{\zeta_i}$, with $d_{\zeta_i} = |\mathbf{x}-\mathbf{x}_{\zeta_i}|$, and, for $\mathbf{x}$ going towards $\mathbf{x}_{\zeta_1}$ or $\mathbf{x}_{\zeta_2}$, $\int_{Z_i} G(\mathbf{x},\mathbf{x}')\,\mathrm{d}\mathbf{x}' \approx P_i/2\pi$.

In these conditions, with $p_{\zeta_i} = p(\mathbf{x}_{\zeta_i})$, one obtains

$$p(\mathbf{x}) = p_0(\mathbf{x}) - \mathrm{i}k\beta\left\langle \frac{Z}{2\pi}\,\frac{\mathrm{e}^{-\mathrm{i}kd_{\zeta_1}}}{d_{.\zeta_1}}, \qquad \frac{Z}{2\pi}\,\frac{\mathrm{e}^{-\mathrm{i}kd_{\zeta_2}}}{d_{\zeta_2}}\right\rangle \begin{Bmatrix} p_{\zeta_1} \\ p_{\zeta_2}\end{Bmatrix}, \tag{8}$$

leading to, when $\mathbf{x}\to\mathbf{x}_{\zeta_1}$ and $\mathbf{x}\to\mathbf{x}_{\zeta_2}$, with $P_i = P\forall i$,

$$P_{\zeta_1} = p_{\zeta_1 0} - \mathrm{i}k\beta\,\frac{P}{2\pi}\,p_{\zeta_1} - \mathrm{i}k\beta\,\frac{Z}{2\pi}\,\frac{\mathrm{e}^{-\mathrm{i}kd_{\zeta_1\zeta_2}}}{d_{\zeta_1\zeta_2}}\,p_{\zeta_2},$$

$$P_{\zeta_2} = p_{\zeta_2 0} - \mathrm{i}k\beta\,\frac{Z}{2\pi}\,\frac{\mathrm{e}^{-\mathrm{i}kd_{\zeta_2\zeta_1}}}{d_{\zeta_2\zeta_1}}\,p_{\zeta_1} - \mathrm{i}k\beta\,\frac{P}{2\pi}\,p_{\zeta_2}.$$

that is,

$$\begin{bmatrix} 1 + \mathrm{i}k\beta P/2\pi & \mathrm{i}k\beta Z/2\pi\ \mathrm{e}^{-\mathrm{i}kd_{\zeta_1\zeta_2}}/d_{\zeta_1\zeta_2} \\ \mathrm{i}k\beta(Z/2\pi)\ \mathrm{e}^{-\mathrm{i}kd_{\zeta_2\zeta_1}}/d_{\zeta_2\zeta_1} & 1 + \mathrm{i}k\beta P/2\pi \end{bmatrix} \begin{Bmatrix} p_{\zeta_1} \\ p_{\zeta_2} \end{Bmatrix} = \begin{Bmatrix} p_{\zeta_1 0} \\ p_{\zeta_2 0} \end{Bmatrix},$$

and the asymptotic form of equation (5) is

$$p_\mu = p_{\mu 0} - \mathrm{i}k\beta \left\langle \frac{Z}{2\pi} \frac{\mathrm{e}^{-\mathrm{i}kd_{\mu\zeta_1}}}{d_{\mu\zeta_1}} \frac{Z}{2\pi} \frac{\mathrm{e}^{-\mathrm{i}kd_{\mu\zeta_2}}}{d_{\mu\zeta_2}} \right\rangle \begin{bmatrix} 1 + \mathrm{i}k\beta \dfrac{P}{2\pi} & \mathrm{i}k\beta \dfrac{Z}{2\pi} \dfrac{\mathrm{e}^{-\mathrm{i}kd_{\zeta_1\zeta_2}}}{d_{\zeta_1\zeta_2}} \\ \mathrm{i}k\beta \dfrac{Z}{2\pi} \dfrac{\mathrm{e}^{-\mathrm{i}kd_{\zeta_2\zeta_1}}}{d_{\zeta_2\zeta_1}} & 1 + \mathrm{i}k\beta \dfrac{P}{2\pi} \end{bmatrix}^{-1} \begin{Bmatrix} p_{\zeta_1 0} \\ p_{\zeta_2 0} \end{Bmatrix}. \tag{9}$$

Equation (9) can be written as $p_\mu = p_{\mu 0} + p_{\mu\zeta}$ where $p_{\mu 0}$ is the "primary" pressure (i.e., in the domain with rigid boundaries) at the microphone location $\mathbf{x}_\mu$ and where $p_{\mu\zeta}$ is the modification to be brought to this pressure in order to take into account the impedances. Note that $p_{\mu\zeta} = \mathbf{a}^{\mathrm{T}} \cdot \mathbf{B}^{-1} \cdot \mathbf{c}$ if $N_\mu = 1$ and $\mathbf{p}_{\mu\zeta} = \mathbf{A} \cdot \mathbf{B}^{-1} \cdot \mathbf{c}$ if not (bold capitals are matrices, bold letters are column vectors). The expression is immediately generalized to N_ζ impedances patches.

Equation (9) is said to be composed of spot measurements because the impedance patches have been reduced to spots through the fact that they possess only one value of the pressure on each. The integral have also been given only one value each, and will later be given the meaning of measurable transfer functions.

2.3.2. *Impedance location optimization and results*

The acoustic level is known from the acoustic pressure at the "microphones". By considering several microphones μ and a number N_ζ of impedances located at $\mathbf{x}_\zeta$, the mean-squared pressure is

$$J(x\zeta) = \| \mathbf{p}_\mu \|^2 = \| \mathbf{p}_{\mu 0} \|^2 + 2\mathscr{R}(\mathbf{p}_{\mu\zeta}{}^* \cdot \mathbf{p}_{\mu 0}) + \| \mathbf{p}_{\mu\zeta} \|^2 = J_\zeta. \tag{10}$$

In this form J is not a sound level but as it is directly related to the sound level, one may take the liberty of calling it the sound level.

Due to interference, J_ζ is greater or less than $J_0 = \| \mathbf{p}_{\mu 0} \|^2$ according to the impedance locations $\mathbf{x}_\zeta$. The analytical form of $\mathbf{p}_{\mu\zeta}$ leads to a closed form of $\{J_{\zeta,\zeta}\}$. Indeed $\{J_{\zeta,\zeta_i}\}$ equals $\{2\mathscr{R}(\mathbf{p}_{\mu\zeta,\zeta_i}{}^* \cdot \mathbf{p}_\mu)\}$ with, of course, $\mathbf{p}_{\mu\zeta,\zeta_i} = \mathbf{A},_{\zeta_i} \cdot \mathbf{B}^{-1} \cdot \mathbf{c} - \mathbf{A} \cdot \mathbf{B}^{-2} \cdot \mathbf{B},_{\zeta_i} \cdot \mathbf{c} + \mathbf{A} \cdot \mathbf{B}^{-1} \cdot \mathbf{c},_{\zeta_i}$. ($\mathbf{a}^*$ is the transpose conjugate of $\mathbf{a}$).

In these conditions, a gradient algorithm gives the locations $\mathbf{x}_\zeta$ which minimize J. This minimization is said to be obtained from an infinity of measurements because $\mathbf{p}_{\mu\zeta}$ is known whatever $\mathbf{x}_\zeta$ from the knowledge of $\mathscr{G}(\mathbf{x}, \mathbf{x}_{\zeta_i})$ and $\mathscr{G}(\mathbf{x}_{\zeta_i}, \mathbf{x}_{\zeta_j})$, whatever $\mathbf{x}_{\zeta_i}$ and $\mathbf{x}_{\zeta_j}$ are.

With nine microphones and from one to ten 20 cm square impedances, and for a wave number equal to 1·6, the optimization tests (without constraints other than a limitation in order for the impedances not to overlap) result in Table 1. Due to the approximation made for the calculation, there are consequences for the geometrical situation at the origin of Table 1. Calculations have been carried out in the 3D half-space by making the acoustic pressure constant on each impedance patch Z_i and by making them very small when seen from the microphones. The source thus must be far from the boundary Γ, where the Z_i are situated, and the same applies to the microphones. Furthermore the control microphones must be far from the source in order for the pressure there to be affected by the presence of the impedances. All these constraints lead to negligible effects of impedance

TABLE 1

Results of the optimization obtained in the academic situation

	$N_\mu = 9,\ J_0 = 4{\cdot}7975 \times 10^{-4}$									
N_ζ	1	2	3	4	5	6	7	8	9	10
Initial x_ζ	3·0	4·0	3·0	2·0	4·0	5·0	5·0	5·0	5·0	5·0
	–	8·0	6·0	7·0	8·0	6·0	6·0	6·0	6·0	6·0
		–	9·0	10·0	10·0	9·0	10·0	10·0	10·0	10·0
			–	13·0	16·0	15·0	15·0	15·0	15·0	15·0
				–	18·0	18·0	18·0	18·0	18·0	18·0
				–	–	20·0	20·0	20·0	20·0	20·0
				–	–	–	22·0	22·0	22·0	22·0
				–	–	–	–	24·0	24·0	24·0
				–	–	–	–	–	26·0	26·0
				–	–	–	–	–	–	28·0
Initial J_ζ	72	76	66	71	73	51	43	45	46	45
Final x_ζ	5·44	5·53	5·53	5·53	5·53	5·53	5·24	5·28	5·28	5·28
	–	5·30	5·28	5·28	5·30	5·28	5·53	5·53	5·53	5·53
	–	–	10·55	10·55	10·55	10·55	10·55	10·55	10·55	10·55
	–	–		17·72	14·70	14·70	14·70	14·70	14·70	14·70
	–	–			17·72	17·72	17·72	17·72	17·72	17·72
	–	–				20·37	20·37	20·37	20·37	20·37
	–	–					22·88	22·64	23·03	22·94
	–	–						23·03	22·64	22·74
	–	–							25·24	25·24
	–	–								27·56
Final J_ζ	61	48	43	40	38	35	33	31	29	26

locations. It is simply required that these effects be visible, as for the time being one is concerned only with the examination of the methodology and of the optimization; the results in dB are of no interest.

In Table 1, $J_0 = \|\mathbf{p}_{\mu 0}\|^2$ is expressed in $(\mathrm{N\,m^{-2}})^2$. The impedance patch locations, of admittance equal to 1, vary along Ox and the coordinates of their centres are given in m. Initial locations are almost arbitrary.

The displacements between initial and final locations may be noticed. For example with four impedances, one of them moves from 13 m to 17·7 m. It is also remarkable that the optimized locations remain stable when the number of impedances is increased. For example from $N_\zeta = 3$ to 10, one of the locations found is always 10·55 m. This could mean that, in the present situation, the inter-influences between patches are negligible. Regarding the values of the mean-squared pressure J_ζ, only the third and the fourth decimals have been written in the table. Despite the fact that the results in dB are of no interest here, two occurrences have to be noted. First, there exist impedance locations which amplify the sound level at the microphones (situation with two impedances located anywhere before optimization). Secondly, it appears in the example that one well located impedance is more efficient than five poorly located impedances, two well located impedances are more efficient than six poorly located impedances, and three well located impedances are more efficient than ten poorly located impedances.

Almost all the technical ingredients needed to deal with the problem of optimizing the impedance locations are now available thanks to the analytical approach. But this latter approach is totally inadequate when dealing with more complicated geometry and to give an idea of the possible order of magnitude for the attenuation in more realistic situations.

With the aim of obtaining information in a cavity, the following section is concerned with a simple case, but now the methods must be able to cope with any geometry.

3. NUMERICAL DESCRIPTION OF A CAVITY WITH IMPEDANCES ON ITS WALLS

3.1. VARIATIONAL FORM AND FINITE ELEMENT DISCRETISATION

A three-dimensional cavity is now under study. Its volume is similar to that with which it is intended to work in the future, and the frequency of concern is around 70 Hz. Before dealing with external sources and vibrating walls, the present chapter sets out to develop the previous technical ingredients with non-vibrating walls and thus with a source inside the cavity. Figure 5 shows the situation. The interior source is arbitrarily situated on the ceiling. The walls are scattered with impedance patches Z_i. For each of them the equation is $\partial_n p(\mathbf{x}) + \mathrm{i}k\beta p(\mathbf{x}) = 0$. The admittance will be the same for every patch and of value 1. Where there is no impedance the walls are described by $\partial_n p(\mathbf{x}) = 0$. The volume where the sound attenuation is sought is called Ω_μ; the subscript indicates that it is the volume of the control microphones. The boundary of the acoustic domain Ω is now $\partial\Omega$.

The direct problem consists here in finding the pressure $p(\mathbf{x})$ which satisfies the following equations: $(\Delta + k^2)p(\mathbf{x}) = g(\mathbf{x}_s)$ with $\mathbf{x} \in \Omega$ and where $\mathbf{x}_s$ is the location of the velocity source; $\partial_n p(\mathbf{x}) = 0$ on $\partial\Omega \backslash Z_t$ where Z_t is the part of the boundary with the impedances; $\partial_n p(\mathbf{x}) + \mathrm{i}k\beta p(\mathbf{x}) = 0$ on Z_t.

For the low frequency range, three methods are in competition to deal with the problem: the modal theory, the boundary integral method and the finite element method. The modal theory will no longer be appropriate once the geometry becomes less regular; the boundary integral method based on boundary integral equations has the great drawback of having to recalculate all the matrices when the frequency changes. For the interior problem, whatever the geometry, the finite element method is arguably the best. However, not keeping the boundary integral method, technically speaking, does not mean that its philosophy cannot be exploited, as will be shown.

The finite element discretizes not the differential equations themselves, but a weak form of them. The associated weak form of the problem is $\langle v, (\Delta + k^2)p(\mathbf{x})\rangle_\Omega = \langle v, g(\mathbf{x}_s)\rangle_\Omega \forall v(\mathbf{x})$, a function belonging to a space function to be defined. The inner product $\langle .,. \rangle_\mathscr{D}$ is in the complex field $\mathbb{C}$. As long as $\langle .,. \rangle_\mathscr{D}$ has a subscript to indicate a domain, it is an inner product; if not $\langle .,. \rangle$ represents a row vector. The weak form merely says that $f(\mathbf{x}) = 0$ in Ω and $\int_\Omega q(\mathbf{x}) f(\mathbf{x})\, \mathrm{d}\mathbf{x} = 0 \forall q(\mathbf{x})$ are equivalent. The weak

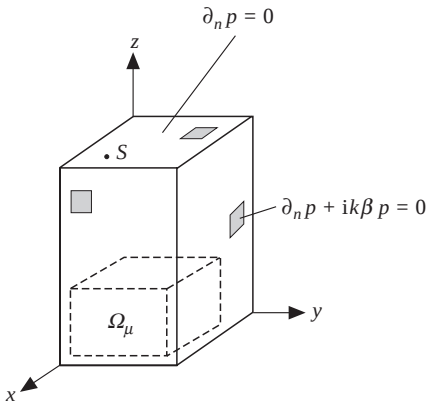

Figure 5. Numerical situation.

form, integrated by parts, reveals some of the boundary conditions. It is called the variational form and is

$$-\langle \nabla v, \nabla p\rangle_\Omega + k^2\langle v, p\rangle_\Omega + \langle v, \partial_n p\rangle_{\partial\Omega} = \langle v, g(\mathbf{x}_s)\rangle_\Omega$$
$$\forall v(\mathbf{x})\in \mathrm{H}^1(\boldsymbol{\Omega}) \quad \text{and} \quad p(\mathbf{x})\in \mathrm{H}^1(\Omega),$$

or

$$-\langle \nabla v, \nabla p\rangle_\Omega + k^2\langle v, p\rangle_\Omega - \mathrm{i}k\beta\langle v, p\rangle_{\partial\Omega} = \langle v, g(\mathbf{x}_s)\rangle_\Omega$$
$$\forall v(\mathbf{x})\in \mathrm{H}^1(\Omega) \quad \text{and} \quad p(\mathbf{x})\in \mathrm{H}^1(\Omega),$$

The variational form can be seen as a variation of the Lagrangian $L = -T + U - W$ (where T, U, W are respectively the kinetic and potential energies, the work of the external conservative forces, expressed in force-like quantities) with the work of the non-conservative forces on the boundary on the right-hand side:

$$-\langle \nabla \delta p, \nabla p\rangle_\Omega + k^2\langle \delta p, p\rangle_\Omega - \langle \delta p, g(\mathbf{x}_s)\rangle_\Omega = +\mathrm{i}k\beta\langle \delta p, p\rangle_{\partial\Omega}$$
$$\forall \delta p(\mathbf{x})\in \mathrm{H}^1(\Omega) \quad \text{and} \quad p(\mathbf{x})\in \mathrm{H}^1(\Omega),$$

The only information given by the function spaces is that the functions must be derivable and integrable.

All the integrals of the variational form are of the following type: $\langle v, u\rangle_{\mathscr{D}} = \int_{\mathscr{D}} v^* u \, \mathrm{d}\mathscr{D}$, where $\mathscr{D}$ represents Ω or $\partial\Omega$. The integrals are calculated piece by piece: i.e.,

$$\int_{\mathscr{D}} v^* u \, \mathrm{d}\mathscr{D} = \sum_{e=1}^{E} \int_{\mathscr{D}_e} v^* u \, \mathrm{d}\mathscr{D}_e \text{ with } \mathscr{D} = \mathscr{D}_1 \cup \mathscr{D}_2 \cup \mathscr{D}_3 \cdots \cup \mathscr{D}_E, \text{ and } \mathscr{D}_i \cap \mathscr{D}_j = \phi.$$

Each elementary domain $\mathscr{D}_e$, called an element, is a simple geometrical form like a segment in 1-D, a triangle or a rectangle in 2-D, a tetrahedron or a hexahedron in 3-D, and the vertices are called nodes. One node usually belongs to several neighbouring elements, except at the corner of the global domain where they are counted only once. (This is a simplified description of the method which is, in fact, far more complex).

Inside each elementary domain $\mathscr{D}_e$, the functions $w(\mathbf{x})$ which are not derivatives are approximated by $w(\mathbf{x}) = \sum_{i=1}^{I} N_i(\mathbf{x})\, w_i$, where i indicates the ith node of the element $\mathscr{D}_e$, which has a total of I nodes. The functions $N_i(\mathbf{x})$ are defined only in $\mathscr{D}_e$, are of value 1 at node i and of value 0 at the other nodes of $\mathscr{D}_e$. They are polynomial. Thus w_i equals $w(\mathbf{x}_i)$ with $\mathbf{x}_i$ the co-ordinates of node i. The $N_i(\mathbf{x})$ are called interpolating nodal functions. This results in

$$\int_{\mathscr{D}_e} v^* u \, \mathrm{d}\mathscr{D}_e = \langle v_j\rangle \int_{\mathscr{D}_e} \{N_j(\mathbf{x})\}\langle N_i(\mathbf{x})\rangle \, \mathrm{d}\mathbf{x}\{u_i\},$$

the integral giving rise to an elementary matrix. When the functions represent derivatives, the derivatives of the interpolating nodal function are under the sign integral. The sum $\sum_{e=1}^{E}$ has its matricial equivalent operation, called assembling, which provides the global matrix.

Here the 3-D rectangular domain is discretized with hexahedric elements with eight nodes, leading to a trilinear interpolation inside each element. The boundary $\partial\Omega$ is thus made up of rectangular faces with a bilinear interpolation. For the sake of simplicity, an absorptive device has the same shape and size as the faces on $\partial\Omega$.

TABLE 2

Comparison between the theoretical and numerical eigenfrequencies situated around 70 Hz

l	m	n	Theoretical eigenfrequencies (Hz)	Numerical eigenfrequencies (Hz)
1	0	1	$f_1 = 61{\cdot}6$	$f_1 = 62{\cdot}3$
0	1	2	$f_2 = 64{\cdot}5$	$f_2 = 65{\cdot}0$
1	1	0	$f_3 = 70{\cdot}8$	$f_3 = 71{\cdot}5$
0	0	3	$f_4 = 72{\cdot}9$	$f_4 = 74{\cdot}2$
1	0	2	$f_5 = 74{\cdot}6$	$f_5 = 75{\cdot}4$
1	1	1	$f_6 = 74{\cdot}9$	$f_6 = 75{\cdot}6$

Inside each elementary domain $\mathscr{D}_e$, the solution is sought in the form

$$p(\mathbf{x}) = \sum_i N_i(\mathbf{x}) p_i,$$

where the interpolating functions $N_i(\mathbf{x})$ are trilinear in the volume and bilinear on the faces, and where the p_i are the nodal values of the pressure.

The matricial form of the discretized variational formulation is now $(-[F] + k^2[G] - \mathrm{i}k\beta[m])\{p\} = \{g\}$ where the addition (or the substraction) of $\mathrm{i}k\beta[m]$ occurs only for the nodes of the faces with impedances and where the columns $\{p\}$ and $\{g\}$ are respectively the nodal values of the pressure and of the excitation.

While the matrices **F** and **G** are built by using a finite element code, the terms of matrix **m**, easily calculated by hand, are directly entered into the code. Indeed, for a sole square element of dimensions $h \times h$, the calculation of $\int_0^h \mathrm{d}x \int_0^h \mathrm{d}y\, N_i(x, y) N_j(x, y)$ with bilinear functions $N_i(x, y)$ results in the matrix

$$[\mathbf{m}] = \begin{bmatrix} 4 & 2 & 1 & 2 \\ 2 & 4 & 2 & 1 \\ 1 & 2 & 4 & 2 \\ 2 & 1 & 2 & 4 \end{bmatrix}.$$

It must be said that the finite element technique is largely used today because it is really efficient without requiring extensive knowledge of mathematics. The price to pay seems to be in the great number of lines in the computer programs.

To illustrate briefly this technique, Table 2 compares eigenfrequency values, in the cavity with perfectly rigid walls, with analytical eigenfrequency values. The numerical resonances were identified by sweeping the frequency and noting the cases where the mean-squared pressure had high values. Care was taken for the source not to be located at a modal node.

3.2. DISCRETIZED INTEGRAL FORMULATION OF THE PROBLEM BY SUBSTRUCTURING

Let $-[F] + k^2[G] = [A_0]$ be the matrix associated with the case of perfectly rigid walls. The equation to be solved is

$$([A_0] - \mathrm{i}k\beta[\mathbf{m}])\{p\} = \{g\}, \quad \text{or} \quad ([I] - \mathrm{i}k\beta[A_0]^{-1}[\mathbf{m}])\{p\} = [A_0]^{-1}\{g\} = -[\mathscr{A}]\{g\} = \{p_0\}.$$

The ith column of the matrix $-\mathscr{A}$ is the response to a unitary excitation applied to the ith component of **g**, inside the cavity with rigid boundaries, $\mathscr{A}$ corresponding to the Green function of the analytical formulation.

As **m** concerns only the nodes of the elements adjacent to a wall, with a face simulating an impedance, while matrix $\mathbf{A}_0$ concerns all the nodes of the cavity, the adding of $\mathrm{i}k\beta\mathbf{m}$

to $\mathbf{A}_0$ has to be taken in the matrix assembling sense. As for the product $\mathbf{A}_0^{-1}\mathbf{m} \equiv -\mathscr{A}\mathbf{m}$, it is a $N_\tau \times N_\gamma$ matrix, where N_τ is the total number of nodes and where N_γ is the number of nodes on the impedances. Clearly $-\mathscr{A}\mathbf{m}$ represents relations between nodes in the cavity and nodes on the absorptive materials whose sense will be given later on. $\mathbf{p}_0$ is the nodal pressure values column vector generated by the excitation, were the walls perfectly rigid.

Upon indexing by ν the nodes on the domain $\Omega \cup \partial\Omega \backslash Z_t$ and as before indexing by γ the nodes on the devices on the domain Z_t, the substructuring used for the problem is

$$\left(\begin{bmatrix} [I_\nu] & [0] \\ [0] & [I_\gamma] \end{bmatrix} + \mathrm{i}k\beta \begin{bmatrix} [\mathscr{A}_{\nu\nu}] & [\mathscr{A}_{\nu\gamma}] \\ [\mathscr{A}_{\gamma\nu}] & [\mathscr{A}_{\gamma\gamma}] \end{bmatrix} \begin{bmatrix} [0] & [0] \\ [0] & [m_{\gamma\gamma}] \end{bmatrix} \right) \begin{Bmatrix} p_\nu \\ p_\gamma \end{Bmatrix} = \begin{Bmatrix} p_{\nu 0} \\ p_{\gamma 0} \end{Bmatrix}. \tag{11}$$

The first matricial line leads to the same form as equation (2) or (4) and, more importantly here, removing $\{p_\gamma\}$ from both matricial lines results in

$$\{p_\nu\} = \{p_{\nu 0}\} - \mathrm{i}k\beta[\mathscr{A}_{\nu\gamma}\mathbf{m}_{\gamma\gamma}]([I_\gamma] + \mathrm{i}k\beta[\mathscr{A}_{\gamma\gamma}\mathbf{m}_{\gamma\gamma}])^{-1}\{p_{\gamma 0}\}. \tag{12}$$

More precisely, with the 'nodal microphones' located inside Ω_μ, i.e., somewhere in $\Omega \cup \partial\Omega \backslash Z_t$, and with μ indexing the nodes of the microphones, the previous equation is

$$\{p_\mu\} = \{p_{\mu 0}\} - \mathrm{i}k\beta[\mathscr{A}_{\mu\gamma}\mathbf{m}_{\gamma\gamma}]([I_\gamma] + \mathrm{i}k\beta[\mathscr{A}_{\gamma\gamma}\mathbf{m}_{\gamma\gamma}])^{-1}\{p_{\gamma 0}\}.$$

When compared with the analytical form

$$p_{\mathbf{x}} \approx p_{\mathbf{x}0} - \mathrm{i}k\beta\langle\mathscr{G}(\mathbf{x}, \mathbf{x}_{\zeta_i})\rangle[I_{ij} + \mathrm{i}k\beta\mathscr{G}(\mathbf{x}_{\zeta_i}, \mathbf{x}_{\zeta_j})]^{-1}\{p_{\zeta_j}0\},$$

the pressure on the microphones in the cavity with rigid walls is recognized as well as the modification brought from the pressure at the impedance locations but without the impedances. Moreover it will be seen that $[\mathscr{G}_{\mu\gamma}] = [\mathscr{A}_{\mu\gamma}\mathbf{m}_{\gamma\gamma}]$ and $[\mathscr{G}_{\gamma\gamma}] = [\mathscr{A}_{\gamma\gamma}\mathbf{m}_{\gamma\gamma}]$ are almost transfer functions between impedances and microphones and auto/inter-influences of the impedances. Such an equation represents the problem with data only from the cavity with rigid boundaries. In fact, the substructuring of the finite element matrix is carried out to obtain the Green function in the cavity with rigid walls, and the elementary function is used in the same way as in the boundary integral equation with a simple layer only.

4. SOUND LEVEL MINIMIZATION FROM A FINITE NUMBER OF MEASUREMENTS

4.1. SIMULATED MEASUREMENTS IN A FINITE ELEMENT MODEL

In the numerical model built here one impedance expands on a face area of an hexahedric element (which has a face on a wall) and is thus described by four nodes. The intention is to use measurements for impedance positioning, among them acoustic pressure where absorptive materials are going to be positioned. Implicitly an impedance location is defined by the co-ordinates of one point, namely the device centre, the dimensions of which are far smaller than the wavelength of the frequency concerned (say a square or circular absorptive device of 0·20 cm side or diameter). Thus only one pressure value, instead of the four values at the four nodes, has to be known.

The choice is between imposing relations on the four nodes before calculation in order to obtain the same value at each node and averaging the four pressure nodal values after calculation. The first approach is inappropriate here as it leads to a combination of a nodal approximation almost everywhere except at the location where the impedance is not yet installed, with a constant value pressure approximation, resulting in the matrix of the cavity with rigid walls which depends on the future impedance location! Such an approach must be abandoned in favour of the second choice. Dealing with mean nodal pressure values where the impedance is going to be located has consequences for the numerical

transfer function between the absorptive device and one interior node (microphone). Other consequences occur in the transfer functions between impedances, i.e., the auto- and inter-influences, and the averaged matrix will be deduced to obtain one value only for the auto and inter-influences. The numerical measurements coming from mean values of matrix or vector components are closely linked to the collocation technique seen during the analytical chapter.

The simplest situation with one microphone and only one device provides the description of the averages required. One begins with

$$p_\mu = p_{\mu 0} - \mathrm{i}k\beta \langle \mathscr{A}_{\mu\gamma} \mathbf{m}_{\gamma\gamma} \rangle ([I_\gamma] + \mathrm{i}k\beta [\mathscr{A}_{\gamma\gamma} \mathbf{m}_{\gamma\gamma}])^{-1} \{p_{\gamma 0}\},$$

also written as

$$p_\mu = p_{\mu 0} - \mathrm{i}k\beta \langle \mathscr{G}_{\mu\gamma} \rangle ([I_\gamma] + \mathrm{i}k\beta [\mathscr{G}_{\gamma\gamma}])^{-1} \{p_{\gamma 0}\},$$

where $N_\mu = 1$ and $N_\gamma = 4$, as a four-node element represents here one impedance.

The matrix $\mathscr{G}_{\mu\gamma}$, the dimensions of which are 1×4, corresponds to the integral $\int_Z G(\mathbf{x}_\mu, \mathbf{x}')\, \mathrm{d}\mathbf{x}'$ seen in the analytical form, expanded at the nodes of the impedance. Naturally the integral is synthesized by adding the distributed values, i.e.,

$$\mathscr{G}_{\mu\zeta} = \sum_{\gamma = 1,4} \mathscr{G}_{\mu\gamma},$$

giving one term only.

The matrix $([I_\gamma] + \mathrm{i}k\beta [\mathscr{G}_{\gamma\gamma}])^{-1}$ originates from $\{p_{\gamma 0}\} = ([I_\gamma] + \mathrm{i}k\beta [\mathscr{G}_{\gamma\gamma}])\{p_\gamma\}$ and corresponds to the term $p_{\zeta 0} = (1 + \mathrm{i}k\beta \int_Z G(\mathbf{x}_\zeta, \mathbf{x}')\, \mathrm{d}\mathbf{x}') p_\zeta$ representing the pressure where the device is to be located, given the pressure at the same place but in the presence of the device.

With

$$p_\zeta = \tfrac{1}{4} \sum_{\gamma = 1,4} p_\gamma,$$

the 4×4 matrix in the factor of $\{p_\gamma\}$ is replaced by the column vector obtained by totalling the four columns. Having in mind the analytical form of the autoinfluence integral at the impedance centre $\mathbf{x}_\zeta$ and with

$$p_{\zeta 0} = \tfrac{1}{4} \sum_{\gamma = 1,4} p_{\gamma 0},$$

one now gives the column vector one value only, equal to the average of its four components. Both previous operations are summed up by totalling all columns and all rows of $([I_\gamma] + \mathrm{i}k\beta [\mathscr{G}_{\gamma\gamma}])$ divided by the matrix dimension, here 4. Such a definition of an average matrix has been used to make the only value $(1 + \mathrm{i}k\beta \mathscr{G}_{\zeta\zeta}) = 1 + \mathrm{i}k\beta \int_Z G(\mathbf{x}_\zeta, \mathbf{x}')\, \mathrm{d}\mathbf{x}'$ correspond to the 4×4 matrix $([I_\gamma] + \mathrm{i}k\beta [\mathscr{G}_{\gamma\gamma}])$. (The identity matrix $[I_\gamma]$ is given the value 1).

A very simple example illustrates what has been just written. The matrix equation is

$$\begin{Bmatrix} p_{10} \\ p_{20} \end{Bmatrix} = \begin{bmatrix} a & b \\ c & d \end{bmatrix} \begin{Bmatrix} p_1 \\ p_2 \end{Bmatrix} = \begin{Bmatrix} ap_1 + bp_2 \\ cp_1 + dp_2 \end{Bmatrix},$$

with p_1 and p_2 replaced by their average value p, the equation is now

$$\begin{Bmatrix} p_{10} \\ p_{20} \end{Bmatrix} = \begin{Bmatrix} (a + b)p \\ (c + d)p \end{Bmatrix},$$

With only the average value $p_0 = (p_{10} + p_{20})/2$ considered, the equality is reduced to $p_0 = [\{(a + b) + (c + d)\}/2]p$. The 2×2 matrix has been replaced by only one value, the sum of its columns and rows and divided by its dimension.

To return to the problem, with one microphone and two impedances the formulation is

$$p_\mu = p_{\mu 0} - \mathrm{i}k\beta\langle\langle \mathscr{A}_{\mu\gamma_1}\rangle[m_{\gamma_1\gamma_1}], \langle \mathscr{A}_{\mu\gamma_2}\rangle[m_{\gamma_2\gamma_2}]\rangle\left(\begin{bmatrix}[I_{\gamma_1}] & [0]\\ [0] & [I_{\gamma_2}]\end{bmatrix}\right.$$

$$\left. + \mathrm{i}k\beta\begin{bmatrix}[\mathscr{A}_{\gamma_1\gamma_1}] & [\mathscr{A}_{\gamma_1\gamma_2}]\\ [\mathscr{A}_{\gamma_2\gamma_1}] & [\mathscr{A}_{\gamma_2\gamma_2}]\end{bmatrix}\begin{bmatrix}[m_{\gamma_1\gamma_1}] & [0]\\ [0] & [m_{\gamma_2\gamma_2}]\end{bmatrix}\right)^{-1}\begin{Bmatrix}p_{\gamma_{10}}\\ p_{\gamma_{20}}\end{Bmatrix},$$

where $[m\gamma_1\gamma_1] = [m_{\gamma_2\gamma_2}] = \mathbf{m}$, leading to

$$p_\mu = p_{\mu 0} - \mathrm{i}k\beta\langle\langle \mathscr{A}_{\mu\gamma_1}\rangle[m_{\gamma\gamma}], \langle \mathscr{A}_{\mu\gamma_2}\rangle[m_{\gamma\gamma}]\rangle\left(\begin{bmatrix}[I_{\gamma_1}] & [0]\\ [0] & [I_{\gamma_2}]\end{bmatrix}\right.$$

$$\left. + \mathrm{i}k\beta\begin{bmatrix}[\mathscr{A}_{\gamma_1\gamma_1}] & [m_{\gamma\gamma}] & [\mathscr{A}_{\gamma_1\gamma_2}] & [m_{\gamma\gamma}]\\ [\mathscr{A}_{\gamma_2\gamma_1}] & [m_{\gamma\gamma}] & [\mathscr{A}_{\gamma_2\gamma_2}] & [m_{\gamma\gamma}]\end{bmatrix}\right)^{-1}\begin{Bmatrix}p_{\gamma_{10}}\\ p_{\gamma_{20}}\end{Bmatrix},$$

In accordance with previous definition, the auto- or inter-influences calculations $\mathscr{G}_{\zeta_i\zeta_j}$ are obtained by the product $[\mathscr{G}_{\gamma_i\gamma_j}] = [\mathscr{A}_{\gamma_i\gamma_j}]\mathbf{m}$ averaged at the end of the operation. The procedure is valid whatever the impedance number. Finally the finite element matrix has been submitted to a substructuring and an averaging to take the form

$$p_\mu = p_{\mu 0} - \mathrm{i}k\beta \underbrace{\langle \mathscr{G}_{\mu\zeta_i}\rangle}_{\dim 1 \times N_\zeta} \underbrace{([I] + \mathrm{i}k\beta[\mathscr{G}_{\zeta_i\zeta_j}])^{-1}}_{\dim N_\zeta \times N_\zeta} \underbrace{\{p_{\zeta_j 0}\}}_{\dim N_\zeta \times 1}. \tag{13}$$

The finite element model is now able to simulate measurements in the following way: (a) the averaged nodal pressure value on an impedance simulates the measurement of the pressure at its centre; (b) the addition of the row vector components representing the transfer function between the device nodes and the microphone simulates the measurement of the transfer function between the device centre and the microphone multiplied by the impedance area; (c) the averaged matrix of the auto- and inter-influences simulates measurements of the auto- and inter-influences multiplied by the impedance area.

In a 3-D rectangular cavity (Ox = 3 m, Oy = 4 m, Oz = 7 m and for a frequency of 69 Hz) the results of such a procedure are in accordance with those directly obtained from the model (with neither substructuring nor averages). For example, Figure 6 shows attenuation over 280 nodes when only one impedance sweeps all of one face of the cavity. It turns out that the arbitrary frequency of 69 Hz is on an anti-resonance but it has been observed that, had the frequency been on a resonance, Figure 6 would have shown great reduction for the impedance on the (modal) anti-node of the pressure mode, in agreement with, for example, references [4, 5].

4.2. ESTIMATES OF THE ACOUSTIC LEVEL AND ITS DERIVATIVES ACCORDING TO THE IMPEDANCE LOCATIONS FOR A 1-D OPTIMIZATION

The whole formulation, both analytical and numerical, has been developed in order to predict what the sound level will be in the presence of impedances, from the knowledge of certain measurements taken in the cavity with rigid walls and of the admittance value.

−0.36	−0.21	−0.09	−0.02	0.005	−0.02	−0.09	−0.18
−0.22	−0.12	−0.05	−0.01	3E-4	−0.009	−0.04	−0.09
−0.08	−0.04	−0.02	−0.003	5E-4	−0.001	−0.01	−0.03
0.05	0.03	0.02	0.01	0.006	0.003	0.001	6E-4
0.08	0.05	0.03	0.02	0.01	4E-4	−0.01	−0.02
−0.03	−0.01	0.004	0.01	0.007	−0.01	−0.04	−0.08
−0.17	−0.09	−0.04	−0.006	5E-4	−0.01	−0.05	−0.11
−0.24	−0.13	−0.05	−0.01	0.001	−0.01	−0.04	−0.09
−0.18	−0.11	−0.04	−6E-4	0.008	5E-4	−0.02	−0.05
−0.05	−0.03	−0.005	0.008	0.01	0.006	5E-4	−0.007
0.02	0.009	0.007	0.006	0.004	0.002	0.001	0.002
−0.03	−0.02	−0.005	−7E-4	6E-5	−0.003	−0.01	−0.02
−0.18	−0.10	−0.03	−0.004	0.002	−0.003	−0.02	−0.06
−0.33	−0.20	−0.07	−0.003	0.01	−0.002	−0.04	−0.10

Figure 6. Attenuation over 280 interior nodes when one impedance sweeps all of one face of the cavity.

The measurements in question are as follows (see Figure 7): the primary pressure field p_{μ_0} at the N_μ control microphones; the primary pressure field at some points $\mathbf{x}_\tau$ located on the wall(s) from which the primary pressure field and its derivatives have to be deduced whatever the point $\mathbf{x}_\zeta$ considered on the wall(s); some transfer functions $G_{\mu\sigma}$ between sources on the wall(s) and the control microphones, from which the transfer functions $G_{\mu\zeta}$ and their derivatives have to be deduced whatever the point $\mathbf{x}_\zeta$ considered on the wall(s); some transfer functions $G_{\sigma\tau}$ between sources and microphones on the wall(s), from which the auto- and inter-influences $G_{\zeta_i\zeta_j}$ and their derivatives have to be deduced whatever the points $\mathbf{x}_{\zeta_i}$ and $\mathbf{x}_{\zeta_j}$ considered on the wall(s).

The functionals J_ζ and $\{J_{\zeta,\zeta}\}$ will then be accessible, given a finite number of measurements.

The quantities deduced from the measurements are estimates calculated from a Taylor series. In 1-D, the method leads to continuous estimates. Only the main features of the method are described here as it has been largely developed in reference [2].

Let a function $f(\mathbf{x})$ be of complex value while the variable $\mathbf{x}$ is in $\mathbb{R}$. In a one-dimensional case the pressure $p_{\zeta 0}(x_\zeta)$, the transfer functions $\mathscr{G}_{\mu\zeta}(x_\mu, x_\zeta)$ (without paying attention to the impedance areas) and the auto-influences (not the inter-influences) $\mathscr{G}_{\zeta\zeta}(x_\zeta, x_\zeta)$ are of this type of function $f(x)$.

Function $f(x)$ is of f_j value when $x = x_j$ for $j = 1, L$. The x_j are at a distance δx_j from x, with $\delta x_j = x - x_j$. The Taylor series is

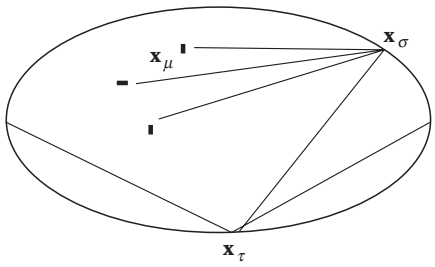

Figure 7. Measurements in the cavity with rigid walls.

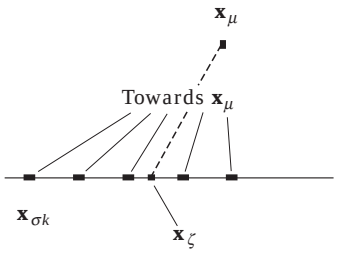

Figure 8. Estimation of the transfer function between one impedance patch and one microphone from sampled transfers.

$$f_j = f(x) - \delta x_j/1! \qquad f_{,x}(x) + \delta x_j^2/2! \qquad f_{,xx}(x) + r_j(\delta x_j),$$

or

$$f_j = \langle f(x), f_{,x}(x), f_{,xx}(x)\rangle \begin{Bmatrix} 1 \\ -\delta x_j \\ \delta x_j^2/2 \end{Bmatrix} + r_j = \mathbf{c}^{\mathrm{T}} \cdot \mathbf{u}_j + r_j.$$

The column $\tilde{\mathbf{c}}$ made up of estimates of $\mathbf{c}$, minimizes the residues r_j. More precisely, $\tilde{\mathbf{c}}$ minimizes a weighted sum of the residues in order to give increasingly greater weight to those sampled values of f the nearer x_j is to x:

$$\min_c \left(\sum_{j=1}^{L} w_j \bar{r}_j r_j \right) = \min_c \left(\sum_{j=1}^{L} w_j \overline{(f_j - \mathbf{c}^{\mathrm{T}} \cdot \mathbf{u}_j)} (f_j - \mathbf{c}^{\mathrm{T}} \cdot \mathbf{u}_j) \right).$$

The minimum value of the quadratic function of $\mathbf{c}$ is reached when the variation is zero, leading to

$$\left(\sum_{j=1}^{L} w_j [\bar{\mathbf{u}}_j \mathbf{u}_j^{\mathrm{T}}] \right) \tilde{\mathbf{c}} = \sum_{j=1}^{L} w_j \bar{\mathbf{u}}_j f_j.$$

Let $\mathscr{G}_{\mu\zeta}(\mathbf{x}_\mu, \mathbf{x}_\zeta)$ take the place of $f(x)$. The role of $\mathbf{x}$ is now played by $\mathbf{x}_\zeta$. The goal is to estimate the values of $\mathscr{G}_{\mu\zeta}$ and $\mathscr{G}_{\mu\zeta,\zeta}$ at $\mathbf{x}_\zeta$. The data available are the K values, called sampled values of the function or sampled data, $\mathscr{G}_{\mu k}(\mathbf{x}_\mu, \mathbf{x}_{\sigma_k})$ when the "source" is located at $\mathbf{x}_{\sigma_k}$. The role of the sampling points x_j in the previous paragraph are now played by the sampling points $\mathbf{x}_{\sigma_k}$.

When one takes into account the weighting window which diminishes the influence of the sampled data $\mathscr{G}_{\mu k}$ the farther $\mathbf{x}_{\sigma_k}$ is from $\mathbf{x}_\zeta$, only the nearest points $\mathbf{x}_{\sigma_k}$ to $\mathbf{x}_\zeta$ need be considered. Figure 8 indicates that the transfer function $\mathscr{G}_{\mu_\zeta}$ and its derivative $\mathscr{G}_{\mu_{\zeta,\zeta}}$ are estimated from the knowledge of the transfer functions $\mathscr{G}_{\mu k}$, named also sampled transfers, at the few points $\mathbf{x}_{\sigma_k}$ in the vicinity of $\mathbf{x}_\zeta$.

With $d_{k\zeta} = \mathbf{x}_\zeta - \mathbf{x}_{\sigma_k}$, the Taylor series is

$$\mathscr{G}_{\mu k} = \mathscr{G}_{\mu_\zeta} - d_{k\zeta}\mathscr{G}_{\mu_{\zeta,\zeta}} + d_{k\zeta^2}/2 \qquad \mathscr{G}_{\mu_{\zeta,\zeta\zeta}} + r_k(d_{k\zeta}).$$

In fact, there are five such equations corresponding to the five points $\mathbf{x}_{\sigma_k}$ nearest to $\mathbf{x}_\zeta$. One can take the liberty of saying that the corresponding values of k are 1 to 5. The weighting window is a triangular window of which the summit is at $\mathbf{x}_\zeta$. The estimates obtained,

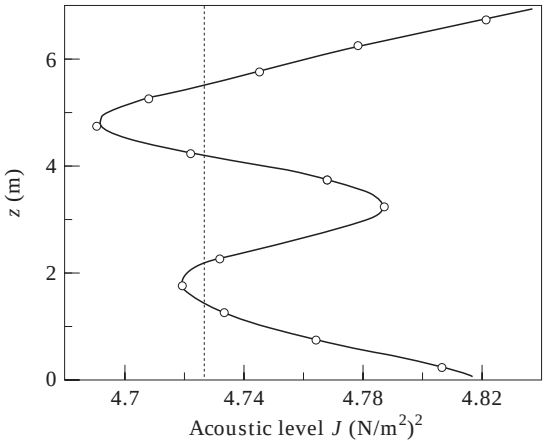

Figure 9. Comparison of the sound level with its estimate. ○, Sampled J; ——, interpolated J; · · · · · · ·, primary field.

presented in a row vector, are $\langle \mathscr{G}_{\mu_\zeta}, \mathscr{G}_{\mu_\zeta,\zeta}, \mathscr{G}_{\mu_\zeta,\zeta\zeta} \rangle$. The calculation of $\mathscr{G}_{\mu_\zeta,\zeta\zeta}$ is of no other use than to increase the accuracy of $\mathscr{G}_{\mu_\zeta,\zeta}$ and, *a fortiori*, on $\mathscr{G}_{\mu_\zeta}$.

By now, everything is ready to work with the functional and its derivatives according to the location of a sole impedance as long as the sampled data—pressures, transfer functions and auto-influences—are taken at the centers of the element faces along a line, here vertical, on a wall of the cavity (here $x = 3$ m, $y = 1{\cdot}25$ m, $L = 14$). The comparison of $J(x_\zeta)$ calculated by the numerical values obtained when the impedance occupies each of the L locations, while $\tilde{J}$ calculated by the estimates from the sampled data, shows good agreement (cf. Figure 9). $\tilde{J}_{,\zeta}$ calculated with the estimates from the sampled data, follows the variations of $\tilde{J}$ (cf. Figure 10).

At this step, with only one impedance patch under study, it is possible to make an attempt to interpret Figures 9 and 10. The acoustic pressure inside the cavity with perfectly rigid walls is established via modes. As the present frequency is at an anti-resonance, there are essentially two modes at work. These modes are silhouetted on the walls and particularly on the line where the absorptive device is to be installed. The impedance acts less efficiently when it is at a weak pressure location. Figure 9 shows places of total

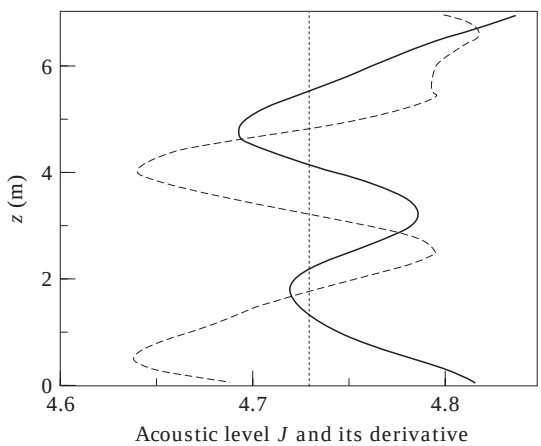

Figure 10. Estimate of the derivative of the sound level. ——, J; - - - -, $J_{,\zeta}$; · · · · · · ·, primary field.

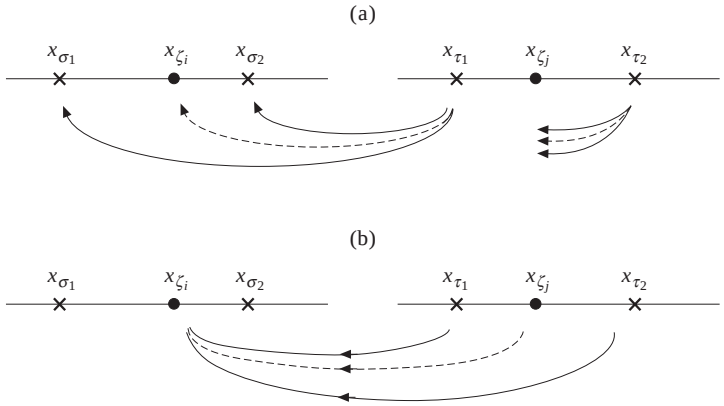

Figure 11. First calculation of the inter-influences' estimates from sampled transfers. (a) First part of the procedure; (b) second part of the procedure.

inefficiency which are the nodes of pressure, taking into account the composition of the two modes. Moreover Figure 10 shows the irregular form of $\tilde{J}_{,\zeta}$ near the ceiling (around $z = 7$ m). As the velocity source is at the ceiling, many evanescent modes exist at this height and the action of the absorptive device is also irregular. This is merely an attempt at interpretation and should not be taken for granted.

For a complex valued function $f(x, y)$ with variables x and y in $\mathbb{R}$, the situation is different. Each of the interinfluences $\mathscr{G}_{\zeta_i\zeta_j}(\mathbf{x}_{\zeta i}, \mathbf{x}_{\zeta j})$ is such a function. Three possible ways of dealing with the estimation shown in reference [7] exist but only one of them gives satisfactory results. Before developing it, notice that the reciprocity principle ought to lead to $\mathscr{G}_{\zeta_i\zeta_j} = \mathscr{G}_{\zeta_j\zeta_i}$, written $\mathscr{G}_{ij} = \mathscr{G}_{ji}$, and $\mathscr{G}_{\zeta_i\zeta_j,\zeta_i} = -\mathscr{G}_{\zeta_i\zeta_j,\zeta_j}$, written $\mathscr{G}_{ij,i} = -\mathscr{G}_{ij,j}$. Here point $\mathbf{x}_{\zeta_i}$ is accompanied by its neighouring sampling points $\mathbf{x}_{\sigma_k}$ with $k = 1, 5$. Similarly point $\mathbf{x}_{\zeta_j}$ is accompanied by the sampling points $\mathbf{x}_{\tau_1}$ with $l = 1, 5$. The sampled values $\mathscr{G}_{\sigma_k\tau_1}(x_{\sigma_k}, x_{\tau_1})$ are among the data from which it is intended to estimate $\mathscr{G}_{\zeta_i\zeta_j}(\mathbf{x}_{\zeta_i}, \mathbf{x}_{\zeta_j})$ and $\mathscr{G}_{\zeta_i\zeta_j\zeta_j}(\mathbf{x}_{\zeta_i}, \mathbf{x}_{\zeta_j})$. One procedure to obtain them could be as follows.

For each of the $\mathbf{x}_\zeta$, i.e., for $l = 1, 5$, the calculation of the estimates carried out as before results in $\langle \mathscr{G}_{il}, \mathscr{G}_{il,i}, \mathscr{G}_{il,ii} \rangle$. From $\mathscr{G}_{il}$ with $l = 1, 5$ the same type of calculation gives $\langle \mathscr{G}_{ij}, \mathscr{G}_{ij,j}, \mathscr{G}_{ij,jj} \rangle$. Figure 11 gives an image of the process when $\mathbf{x}_{\zeta_i}$ and $\mathbf{x}_{\zeta_j}$ are each accompanied by two sampling points only, in order to make the figure easier to read. Graph(a) shows the estimation of $\mathscr{G}_{il} = \mathscr{G}_{\zeta_i\tau_1}(x_{\zeta_i}, x_{\tau_1})$ in a dotted line, from $\mathscr{G}_{\sigma_1\tau_1}$ and $\mathscr{G}_{\sigma_2\tau_1}$ in a continuous line, which could be named "first-hand data". In the same way $\mathscr{G}_{i2} = \mathscr{G}_{\zeta_i\tau_2}(\mathbf{x}_{\zeta_i}, \mathbf{x}_{\tau_2})$ would be obtained. Graph (b) shows the estimation $\mathscr{G}_{ij} = \mathscr{G}_{\zeta_i\zeta_j}(x_{\zeta_i}, x_{\zeta_j})$ in a dotted line, from $\mathscr{G}_{i1}$ and $\mathscr{G}_{i2}$ now available, and which could be named "second-hand data".

Another procedure of estimation of the inter-influence between impedance patches could also be as follows.

For each of the $\mathbf{x}_{\sigma_k}$, i.e., for $k = 1, 5$ the calculation of the estimates carried out as before results in $\langle \mathscr{G}_{kj}, \mathscr{G}_{kj,j}, \mathscr{G}_{kj,jj} \rangle$. From $\mathscr{G}_{kj}$ with $k = 1, 5$ the same type of calculation gives $\langle \mathscr{G}_{ij}, \mathscr{G}_{ij,i}, \mathscr{G}_{ij,ii} \rangle$. Figure 12 gives an idea of the process, if points $\mathbf{x}_{\zeta_i}$ and $\mathbf{x}_{\zeta_j}$ had had only two sampling points. Graph (a) shows the estimation of $\mathscr{G}_{1j} = \mathscr{G}_{\sigma_1\zeta_j}(x_{\sigma_1}, x_{\zeta_j})$ from first-hand data and graph (b) shows the estimation of $\mathscr{G}_{ij}$ from second-hand data made up of $\mathscr{G}_{kj}$, $k = 1, 2$.

The expected equality $\mathscr{G}_{ij} = \mathscr{G}_{ji}$ can be well observed, but the expected equality $\mathscr{G}_{ij,i} = -\mathscr{G}_{ij,j}$ less so. However, one of the derivatives is always better than the other. In the situation of Figure 13, one impedance z_2 sweeps the line while another, called z_1, is

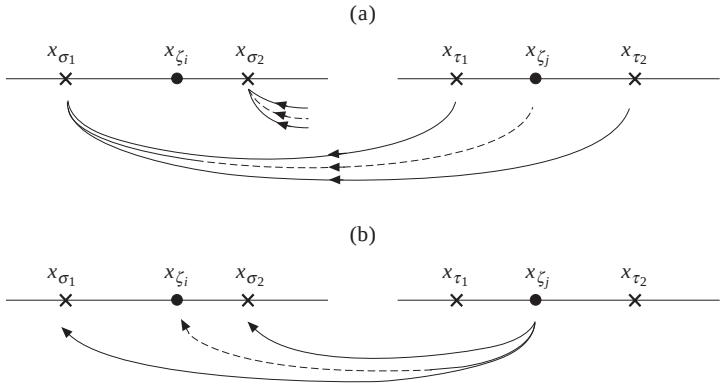

Figure 12. Second calculation of the inter-influences' estimates from sampled transfers. (a) First part of the procedure; (b) second part of the procedure.

fixed on the line but outside a sampling point. No exact value of the inter-influence exists. That is why Figure 13 compares the estimate of the inter-influence between both impedances with the known inter-influence between the sampling points and the one nearest to Z_2. With a larger number of sampling points, the one nearest to Z_2 is still nearer to Z_2 and the comparison between the estimate of the inter-influence and the known value of it are in good agreement (cf. Figure 14). Figure 15 shows that one of the derivatives is better than the other.

4.3. 1-D LOCATION OPTIMIZATION AND RESULTS

The problem consists in finding the optimal locations for one or more impedances along a line on a wall of the cavity.

Numerical sampling data to play the role of measurements are recorded.

The nodal pressures $\{p_{\gamma 0}\}$ are first recorded and they are given their associated measured pressures $\{p_{\zeta 0}\}$. In the present situation, the number of nodes concerned by the sampling locations of the impedances is $N_\gamma = 30$ and the number of sampling centre locations is $N_\zeta = 14$. In the future a refined mesh will increase N_γ (typically 200) to improve the

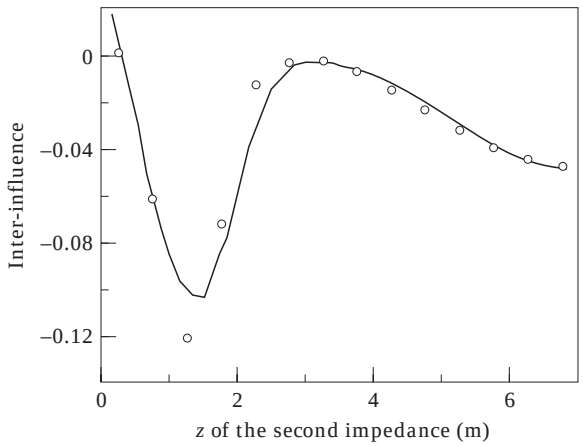

Figure 13. Graph of the estimate of $\mathscr{G}_{ij}$ from 14 sampled data. ○, Sampled G_{12}; ——, estimated G_{12}. First impedance at $z = 1{\cdot}33$.

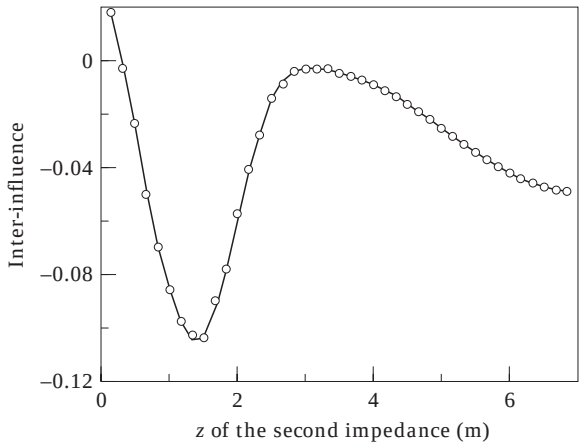

Figure 14. Graph of the estimate of $\mathscr{G}_{ij}$ from 41 sampled data. Key as Figure 13, First impedance at $z = 1{\cdot}33$.

numerical approximation while the goal is to use the smallest possible number of measurements N_ζ (typically 10).

$[\mathscr{G}_{\mu\gamma}]$ is not recorded explicitly. The $N_\zeta = 14$ sampling points, representing the impedance centres, being chosen, the matrix $[\mathscr{G}_{\mu\gamma}]$ is built from $[A_0^{-1}]$ by extracting the $N_\mu \times 4$ matrices $[\mathscr{A}_{\mu\gamma_i}]$, each of them describing the relation between the control microphones and the 4 nodes of one impedance with center ζ_i. Then each $[\mathscr{A}_{\mu\gamma_i}]$ is multiplied by **m** and the result is summed up for each microphone to represent the transfer function (multiplied by the impedance area). All the synthesized transfer functions are organised to obtain the measurements $[\mathscr{G}_{\mu\zeta}]$. Here $N_\mu = 1$ or 8 or 280 or 945 and $N_\gamma = 30$ while $N_\zeta = 14$.

$[\mathscr{G}_{\gamma\gamma}]$ is not recorded explicitly either. The 4×4 matrix $[\mathscr{A}_{\gamma_i\gamma_j}]$ is extracted from $[A_0^{-1}]$ and describes the relation between the 4 nodes of one impedance with centre ζ_i, and the 4 nodes of impedance with centre ζ_j. Then $[\mathscr{A}_{\gamma_i\gamma_j}]$ is multiplied by **m**. Finally the average value of this matrix leads to the matrix of measurements $[\mathscr{G}_{\zeta_i\zeta_j}]$. All the measurements are organised into the matrix $[\mathscr{G}_{\zeta\zeta}]$.

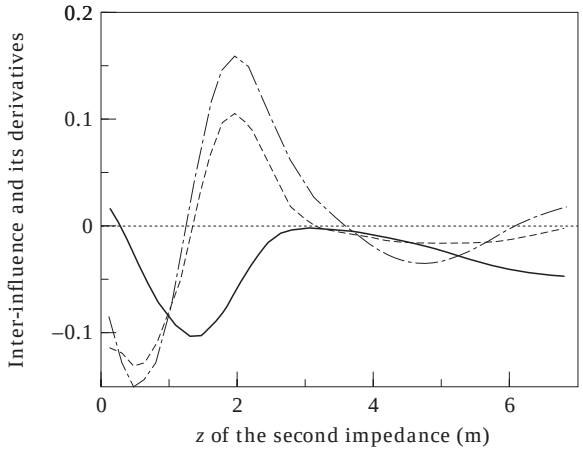

Figure 15. Graph of the estimates of $\mathscr{G}_{ij,i}$ and $\mathscr{G}_{ij,j}$. ——, G_{12}; - - - -, $G_{12,2}$; ·—·—·, $-G_{12,1}$. First impedance at $z = 1{\cdot}33$.

TABLE 3

Results of the optimization for one impedance patch with 280 *observation points*

Initial z_ζ	4·1	2·1
Final z_ζ	4·83	1·79
J	4·6921	4·7191

The measurements obtained are the inputs of the calculations of the estimates made during minimisation by a gradient algorithm.

The optimisation occurs under a constraint of non-overlapping, in order for the impedances to be well differentiated from each other or, at worst, juxtaposed. Each patch measures 0·5 m × 0·5 m. The admittance is equal to 1 and the frequency is 69 Hz.

4.3.1. *Optimization of only one impedance*; Table 3

The situation is the same as that shown in Figures 9 and 10. No inter-influence exists and the descent algorithm is applied with $N_\mu = 280$ and on the line $x = 3$ m, $y = 1{\cdot}25$ m. In Figures 9 and 10, the minima are approximately $z = 1{\cdot}75$ m and $z = 4{\cdot}80$ m. Table 3 shows that $z = 4{\cdot}83$ m when the initial location is 4·1 m and $z = 1{\cdot}79$ m when the initial location is 2·1 m. The final values of J_ζ are those of Figures 9 and 10.

4.3.2. *Optimization at one point* ($N_\mu = 1$) (*optimisation on the line* $x = 3$ m *and* $y = 0{\cdot}25$ m); Table 4

In Table 4, for $N_\zeta = 1$, the initial impedance location is arbitrarily at $z = 1$ m, leading to the final location at $z = 0{\cdot}25$ m. This final location gives one an idea of what the initial locations for two patches could be. They move from (1 m, 2 m) to (0·25 m, 0·75 m). Thus the initial locations are not totally arbitrary. The case of $N_\zeta = 14$ is of no interest here regarding the optimization as the entire line is covered with impedances, but it does show that this does not give the greatest attenuation.

Table 4 reminds one that some locations increase J_0 ($N_\zeta = 2$ with 1 m and 2 m as initial locations) and also provides two important pieces of information. From $N_\zeta = 3$ to 9, two favourable zones for attenuation seem to appear, one at about 0·85 m, where the impedances gather, and the other at around 6 m where another group of impedances gathers. As soon as $N_\zeta \geqslant 10$, the patches are inevitably outside these favourable zones with the consequence that the attenuation decreases. The optimum is reached with $N_\zeta = 9$ where the best attenuation is of approximatley 4·5 dB.

4.3.3. *Optimization at a microphone antenna* ($N_\mu = 8$) (*line* $x = 3$ m *and* $y = 0{\cdot}25$ m); Table 5

In Table 5, two initial situations amplify J_0 ($N_\zeta = 12$ and 13). The case $N_\zeta = 13$ is not changed into an attenuation by the optimization but the amplification is slightly reduced. When $N_\zeta = 14$, J_ζ has the same value as J_0 and the 14 patches are totally inefficient.

Beyond $N_\zeta = 5$ the attenuation decreases. If what has been said in the previous paragraph is true, only one favourable zone could possibly exist here in the neighborhood of 2·5 m.

When the number of observation points, i.e., the number of control microphones, increases, it is more difficult to obtain a significant attenuation. The optimum at $N_\zeta = 5$ is only of approximately 1·4 dB.

The reader will notice that the initial locations often are well situated due to experience which makes one choose the initial locations from the preceding final locations as above.

4.3.4. *Optimization over one third of the domain* ($N_\mu = 280$, *here the domain* Ω_μ *does not have its base on* $x0y$) (*line* $x = 3$ m *and* $y = 0{\cdot}25$ m); Table 6

Table 6 shows that almost all the initial locations amplify J_0 (with 14 impedances, the sound level in the cavity with rigid walls is amplified up to 1·7 dB). From among them, only the case where $N_\zeta = 8$ is not changed into an attenuation. Beyond $N_\zeta = 8$, the calculation time is really long.

The optimal situation is with $N_\zeta = 6$, giving an attenuation of 0·22 dB. Two groups of impedances are visible, around 0·75 m and around 5·6 m. They already appear at $N_\zeta = 4$.

4.3.5. *Optimization over the entire domain* ($N_\mu = 945$) (*line* $x = 3$ m *and* $y = 0{\cdot}25$ m); Table 7

Here again two groups of impedances, at 1·8 m and at 4·7 m, allow one to obtain an optimal attenuation of 0·1 dB with $N_\zeta = 4$. This miniscule attenuation comes from taking into consideration the whole volume of the cavity in the minimization of the acoustic level. Beyond $N_\zeta = 7$, locations are not given in Table 7 due to the long calculation time.

TABLE 4

Results of the optimization for impedance patches with 1 *observation point*

	$N_\mu = 1$, $J_0 = 1{\cdot}8726 \times 10^{-2}$ (N/m^2)^2													
N_ζ	1	2	3	4	5	6	7	8	9	10	11	12	13	14
Initial z_ζ	1·0	1·0	0·5	0·5	0·25	0·25	0·25	0·25	0·25	0·25	0·25	0·25	0·25	0·25
	–	2·0	1·0	1·0	0·75	0·75	0·75	0·75	0·75	0·75	0·75	0·75	0·75	0·75
	–	–	1·5	1·5	1·25	1·25	1·25	1·25	1·25	1·25	1·25	1·25	1·25	1·25
	–	–	–	5·0	5·0	3·0	2·0	1·75	1·75	1·75	1·75	1·75	1·75	1·75
	–	–	–	–	6·0	5·0	3·5	3·0	4·5	3·0	3·0	2·75	2·3	2·25
	–	–	–	–	–	6·0	5·0	4·0	5·0	4·75	4·25	3·75	3·0	2·75
	–	–	–	–	–	–	6·0	5·0	5·5	5·25	4·75	4·25	3·75	3·25
	–	–	–	–	–	–	–	6·0	6·0	5·75	5·25	4·75	4·25	3·75
	–	–	–	–	–	–	–	–	6·50	6·25	5·75	5·25	4·75	4·25
	–	–	–	–	–	–	–	–	–	6·75	6·25	5·75	5·25	4·75
	–	–	–	–	–	–	–	–	–	–	6·75	6·25	5·75	5·25
	–	–	–	–	–	–	–	–	–	–	–	6·75	6·25	5·75
	–	–	–	–	–	–	–	–	–	–	–	–	6·75	6·25
	–	–	–	–	–	–	–	–	–	–	–	–	–	6·75
Initial att. (dB)	0·31	−0·01	1·41	1·96	2·87	2·02	2·14	1·53	4·36	3·63	3·41	2·98	1·77	1·40
Final z_ζ	0·25	0·25	0·25	0·25	0·25	0·25	0·25	0·25	0·25	0·25	0·25	0·25	0·25	0·25
	–	0·75	0·75	0·75	0·75	0·75	0·75	0·75	0·75	0·75	0·75	0·75	0·75	0·75
	–	–	1·25	1·25	1·25	1·25	1·25	1·25	1·25	1·25	1·25	1·25	1·25	1·25
	–	–	–	5·26	5·43	5·10	1·75	1·75	1·75	1·75	1·75	1·75	1·75	1·75
	–	–	–	–	6·0	5·61	5·33	5·04	4·75	4·25	3·75	2·47	2·25	2·25·
	–	–	–	–	–	6·18	5·83	5·54	5·25	4·75	4·25	3·75	3·01	2·75
	–	–	–	–	–	–	6·35	6·04	5·75	5·25	4·75	4·25	3·75	3·25
	–	–	–	–	–	–	–	6·54	6·25	5·75	5·25	4·75	4·25	3·75
	–	–	–	–	–	–	–	–	6·75	6·25	5·75	5·25	4·75	4·25
	–	–	–	–	–	–	–	–	–	6·75	6·25	5·75	5·25	4·75
	–	–	–	–	–	–	–	–	–	–	6·75	6·25	5·75	5·25
	–	–	–	–	–	–	–	–	–	–	–	6·75	6·25	5·75
	–	–	–	–	–	–	–	–	–	–	–	–	6·75	6·25
	–	–	–	–	–	–	–	–	–	–	–	–	–	6·75
Final att. (dB)	0·72	1·55	2·00	2·47	3·02	3·56	4·07	4·09	4·48	4·32	3·86	3·05	1·79	1·40

TABLE 5

Results of the optimization for impedance patches with eight observation points

	$N_\mu = 8$, $J_0 = 2{\cdot}4887 \times 10^{-1}$ (N/m^2)^2													
N_ζ	1	2	3	4	5	6	7	8	9	10	11	12	13	14
Initial z_ζ	4·0	2·0	2·0	2·0	2·0	1·5	1·0	1·0	1·0	1·0	1·0	0·8	0·3	0·25
	–	4·0	2·5	2·5	2·5	2·0	1·5	1·5	1·5	1·5	1·5	1·3	0·8	0·75
	–	–	3·0	3·0	3·0	2·5	2·0	2·0	2·0	2·0	2·0	1·8	1·3	1·25
	–	–	–	3·5	3·5	3·0	2·5	2·5	2·5	2·5	2·5	2·4	1·9	1·75
	–	–	–	–	4·0	3·5	3·0	3·0	3·0	3·0	3·0	2·9	2·4	2·25
	–	–	–	–	–	4·0	3·5	3·5	3·5	3·5	3·5	3·5	3·0	2·75
	–	–	–	–	–	–	4·0	4·0	4·0	4·0	4·0	4·0	3·5	3·25
	–	–	–	–	–	–	–	4·5	4·5	4·5	4·5	4·6	4·1	3·75
	–	–	–	–	–	–	–	–	5·0	5·0	5·0	5·1	4·6	4·25
	–	–	–	–	–	–	–	–	–	5·5	5·5	5·6	5·2	4·75
	–	–	–	–	–	–	–	–	–	–	6·0	6·2	5·75	5·25
	–	–	–	–	–	–	–	–	–	–	–	6·7	6·25	5·75
	–	–	–	–	–	–	–	–	–	–	–	–	6·75	6·25
	–	–	–	–	–	–	–	–	–	–	–	–	–	6·75
Initial att. (dB)	0·03	0·23	1·81	1·31	1·29	1·39	1·02	1·13	0·89	0·63	0·29	−0·13	−0·86	0·00
Final z_ζ	2·67	2·44	2·15	2·00	1·65	1·50	1·05	1·01	1·13	1·02	1·41	1·02	0·77	0·25
	–	2·94	2·65	2·50	2·15	2·00	1·55	1·51	1·63	1·52	1·91	1·52	1·27	0·75
	–	–	3·15	3·00	2·65	2·50	2·05	2·01	2·13	2·02	2·41	2·02	1·77	1·25
	–	–	–	3·50	3·15	3·00	2·55	2·51	2·63	2·52	2·91	2·52	2·27	1·75
	–	–	–	–	3·65	3·50	3·05	3·01	3·13	3·02	3·41	3·01	2·77	2·25·
	–	–	–	–	–	4·00	3·55	3·51	3·63	3·52	3·91	3·51	3·27	2·75
	–	–	–	–	–	–	4·05	4·01	4·13	4·02	4·41	4·01	3·76	3·25
	–	–	–	–	–	–	–	4·51	4·63	4·52	4·91	4·51	4·26	3·75
	–	–	–	–	–	–	–	–	5·13	5·02	5·41	5·01	4·76	4·25
	–	–	–	–	–	–	–	–	–	5·52	5·91	5·53	5·26	4·75
	–	–	–	–	–	–	–	–	–	–	6·41	6·12	5·75	5·25
	–	–	–	–	–	–	–	–	–	–	–	6·70	6·25	5·75
	–	–	–	–	–	–	–	–	–	–	–	–	6·75	6·25
	–	–	–	–	–	–	–	–	–	–	–	–	–	6·75
Final att. (dB)	0·31	0·82	1·21	1·32	1·44	1·39	1·02	1·13	0·91	0·61	0·33	0·10	−0·46	0·00

5. SUMMARY AND CONCLUSION

With a view to the passive acoustic control of the sound level in the satellite compartment of the Ariane 5 launcher, this paper is an introduction to the original question of how to optimize impedance locations on the walls of an acoustic cavity. The introductory investigation was made in two steps: an analytical formulation of an academic situation followed by a numerical formulation in a 3-D rectangular cavity.

In a half-space limited by a perfectly rigid boundary, the Helmholtz equation and Sommerfeld radiation condition govern the acoustic solution. Let $G(\mathbf{x}, \mathbf{x}')$ and $p_{\mu 0}$ be the elementary solution with the rigid boundary and the acoustic pressure at a "microphone" located at $\mathbf{x}_\mu$. With one impedance only, the pressure becomes $p_\mu = p_{\mu 0} + p_{\mu\zeta}$ where $p_{\mu\zeta}$ is a modification added to $p_{\mu 0}$ in order to take into account the impedance. This modification has an asymptotic form when the microphone is sufficiently far from the boundary and thus also far from the impedance situated at $\mathbf{x}_\zeta$. The acoustic level is written $J(\mathbf{x}_\zeta) = |p_\mu|^2 = J_0 + 2\mathscr{R}\,(p^*_{\mu\zeta} \cdot p_{\mu 0}) + |p_{\mu\zeta}|^2$.

TABLE 6

Results of the optimization for impedance patches with 280 *observation points*

	$N_\mu = 280$, $J_0 = 3{\cdot}7995$ $(\mathrm{N/m^2})^2$							
N_ζ	1	2	3	4	5	6	7	8
Initial z_ζ	4·0	4·0	2·0	1·0	1·5	1·3	1·3	1·3
	–	6·0	4·0	2·0	2·5	1·8	1·8	1·8
	–	–	6·0	4·0	4·4	2·5	2·8	2·5
	–	–	–	6·0	4·95	3·5	3·5	3·5
	–	–	–	–	5·5	4·5	4·5	4·5
	–	–	–	–	–	5·0	5·0	5·0
	–	–	–	–	–	–	5·5	5·5
	–	–	–	–	–	–	–	6·2
Initial att. (dB)	−0·1	−0·19	−0·19	−0·21	0·17	−0·23	−0·14	−0·34
Final z_ζ	0·25	0·25	0·25	0·25	0·25	0·25	0·25	0·25
	–	0·75	0·75	0·75	0·75	0·75	0·75	0·75
	–	–	1·25	1·25	1·25	1·25	1·25	1·25
	–	–	–	5·26	5·43	5·10	1·75	1·75
	–	–	–	–	6·00	5·61	5·33	5·04
	–	–	–	–	–	6·18	5·83	5·54
	–	–	–	–	–	–	6·35	6·04
	–	–	–	–	–	–	–	6·54
Final att. (dB)	0·07	0·17	0·18	0·19	0·19	0·22	0·13	−0·06

Due to interferences, J_ζ is greater or less than J_0 according to the impedance location. Thanks to the closed form of $p_{\mu\zeta}$, $J_{\zeta,\zeta}$ is analytically available, and a conventional descent algorithm gives the minima. With still one microphone but more than one impedance,

TABLE 7

Results of the optimization for impedance patches with 945 *observation points*

	$N_\mu = 945$, $J_0 = 21{\cdot}0614$ $(\mathrm{N/m^2})^2$						
N_ζ	1	2	3	4	5	6	7
Initial z_ζ	4·0	4·0	2·0	2·0	2·0	1·0	1·0
	–	5·0	4·4	3·0	3·0	2·0	2·0
	–	–	5·1	4·4	4·4	3·0	3·0
	–	–	–	5·1	5·1	4·4	4·0
	–	–	–	–	5·7	5·1	4·6
	–	–	–	–	–	5·7	5·2
	–	–	–	–	–	–	5·8
Initial att. (dB)	−0·08	0·00	0·06	−0·17	−0·20	−0·25	−0·34
Final z_ζ	4·75	4·51	1·82	1·45	1·75	1·46	1·13
	–	5·01	4·55	1·95	4·01	1·96	1·63
	–	–	5·05	4·55	4·51	4·02	2·13
	–	–	–	5·05	5·00	4·52	3·99
	–	–	–	–	5·50	5·02	4·49
	–	–	–	–	–	5·52	4·99
	–	–	–	–	–	–	5·49
Final att. (dB)	0·04	0·09	0·10	0·11	0·09	0·08	0·01

interactions between impedances occur. It has been observed that the impedances gather at the preceding minima. Finally a table shows the results for an antenna made up of nine microphones and for 1 to 10 impedances.

The first step, important in expliciting the methodology, cannot give any realistic order of magnitude concerning the results. It now requires a numerical model dealing with a less academic situation yet still following the analytical methodology, to provide information about possible attenuations.

A 3-D rectangular acoustic cavity is described by the finite element method. With rigid walls, the Helmholtz equation only governs the solution as rigid boundary conditions are natural in the variational form. Nodal approximation leads to the numerical solution. If $\mathbf{A}_0$ is the finite element matrix with rigid walls, $\mathscr{A} = -\mathbf{A}_0^{-1}$ plays the role of the elementary function of the interior problem. Let $p_{\Omega 0}$ be the nodal solution, in particular at certain nodes called microphones. With some impedances on the walls of the cavity, the pressure becomes $p_\Omega = p_{\Omega 0} + p_{\Omega\zeta}$ where the modification $p_{\Omega\zeta}$ to be made develops as in the analytical case thanks to a particular substructuring of the finite element matrix. The effects of one impedance sweeping the entire surface of a wall have been shown, focusing on a particular line on the wall for the 1-D optimization.

When speaking of data or measurements, it is implicitly understood that spot items are used, while numerical modelling is based essentially on elements. A definition of numerical measurements has to be given. To this end, imposing relations between the four nodes of an element describing an impedance to obtain only one pressure value on it, has been shown to give very poor results. The choice of an averaged value of the four nodes has proved to be very efficient. So now, the whole analytical formulation can be used.

Also thanks to the numerical averages used to define some measurements, an estimation procedure was carried out leading to the modification $p_{\Omega\zeta}$ whatever the impedance locations. The functionals J_ζ and $\{J_\zeta\}$ are determined from the following limited number of measurements: the primary field $p_{\mu 0}$ at the control microphones; the primary field $p_{\tau 0}$ at some points on the walls of the cavity; some transfer functions $G_{\mu\sigma}$ between sources on the walls and control microphones; some transfer functions $G_{\sigma\tau}$ between sources and microphones on the walls. The 1-D optimization is obtained here also by a gradient algorithm. Within severe conditions (room of 84 m^3, frequency of 69 Hz at an anti-resonance, 1-D optimization on one line on one wall of the cavity), the order of magnitude obtained to date is as follows: 4 dB at one microphone; 1·4 dB on an antenna made up of eight microphones; 0·2 dB for around one third of the cavity volume (280 microphones); 0·1 dB for the entire cavity volume (945 microphones).

It has constantly been noticed that too many impedances prevent any attenuation, and it seems that a phenomenon of impedance grouping exists.

The 1-D optimization results are currently under study to associate a modal interpretation. A flexible wall submitted to an external plane wave will then be considered to optimize the insulation of the walls by impedances inside the cavity. Finally a 2D optimization has to be envisaged in a more appropriate geometry for our ends.

ACKNOWLEDGMENT

We wish to express our gratitude to the members of the vibro-acoustic team organised by the CNES for supporting this study.

REFERENCES

1. V. MARTIN, PH. VIGNASSA and B. PESEUX 1994 *Journal of Sound and Vibration* **176**, 307–332. Numerical vibro-acoustic modelling of aircraft for the active acoustic control of interior noise.
2. B. NAYROLES, G. TOUZOT and P. VILLON 1994 *Journal of Sound and Vibration* **171**, 1–21. Using diffuse approximation for optimizing the locations of antisound sources.
3. E. BENZARIA and V. MARTIN 1994 *Journal of Sound and Vibration* **173**, 137–144. Secondary source locations in active noise control: selection or optimization?
4. A. DORIA 1995 *Journal of Sound and Vibration* **181**, 673–685. Control of acoustic vibrations of an enclosure by means of multiple resonators.
5. A. CUMMINGS 1992 *Journal of Sound and Vibration* **154**, 25–44. The effects of a resonator array on the sound field in a cavity.
6. V. MARTIN 1995 in *The Proceedings of Internoise*'95; New York: The International Congress on Noise Control Engineering, Noise Control Foundation, 549–552. Impedance locations on a rigid boundary: simulated 1D optimization from sampled data.
7. V. MARTIN 1995 (*juin*) *Rapport intermédiaire de contrat CNES* n°94/CNES/3133. Positionnement d'impédances sur un plan réfléchissant: optimisation 1D à partir de données échantillonnées.
8. V. MARTIN and A. BODRERO 1995 (septembre) *Rapport de fin de contrat* CNES n°94/CNES/3133. Positionnement d'impédances sur un plan réfléchissant: optimisation 1D à partir de données échantillonnées.